CHAPTER 4

Performance Evaluation of Downlink Power Allocation Mechanisms for Soft Handoff in the WCDMA System with Power Control Errors

Soft handoff is a crucial technique for code division multiple access (CDMA) systems to provide smooth and seamless real time multimedia services in wireless networks. Soft handoff allows a mobile terminal to establish communication links to more than one base station simultaneously, thereby improving the signal quality [33] [34] [12]. However, soft handoff may also decrease system capacity or introduce more interference to other users because of assigning multiple channels to one mobile station.

Because the performance of CDMA systems is interference-limited, it is important to design a proper power allocation scheme for soft handoff to control the amount of transmission power. In the literature, some downlink power allocation schemes have been proposed for soft handoff in CDMA systems, including equal power allocation (EPA) [20] [21] [22], quality balancing power allocation (QBPA) [23], site selection diversity transmission (SSDT) [14] [15], and link proportional power allocation (LPPA) [18] [19]. Traditionally, the SSDT scheme, which selects the best base station to transmit signals to the user, has been shown by simulation as the optimal

solution for downlink power allocation in soft handoff from the standpoint of power efficiency.

However, the performance of downlink power allocation mechanisms in soft handoff can be strongly influenced by transmit power control errors. In addition to power control errors, base station power shortage is another factor causing performance outage during soft handoff in CDMA systems. To our knowledge, the analysis of the joint effects of power control error and power shortage on downlink power allocation mechanisms in soft handoff is still lacking in the literature. The objective of this chapter and [35] is to develop such an analytical method. We will incorporate the above two factor in our analytical model. The contribution of this work are three folds. First, we apply a harmonic-arithmetic mean inequality and Chebyshev inequality to prove that SSDT is the most efficient power allocation mechanism as compared to other schemes, such as EPA, QBPA, and LPPA schemes. Secondly, we further derive the closed-form expressions for the outage probabilities of different power allocation mechanisms subject to transmission power control errors. Third, from both the perspectives of base station power shortage and power control errors, we develop a semi-analytical approach to evaluate the outage performance of different power allocation schemes. From our numerical results, we find that LPPA exhibits the lowest outage probability compared to SSDT and EPA when the traffic load is not heavy, while SSDT is the best choice with a heavy traffic load.

The rest of this chapter is organized as follows. Section 4.1 describes the four considered power allocation schemes, including LPPA, SSDT, QPA and QBPA. Section 4.2 compares the power efficiency of the four power allocation schemes. Section 4.3 analyzes the impact of power control errors. Section 4.4 gives some numerical results and discusses the effect of base station power shortage and transmission power control errors. We give our concluding remarks in Section 4.5.

4.1 Downlink Power Allocation Strategies

A downlink soft handoff process requires multiple base stations to simultaneously allocate power to a mobile terminal during handoff. There are four downlink power allocation strategies considered in this chapter, including (1) link proportional power allocation (LPPA), (2) equal power allocation (EPA), (3) quality balancing power allocation (QBPA), and (4) site selection diversity transmission (SSDT). In this section, we will detail the principles of each method. To begin with, we discuss how to calculate signal-to-interference ratio (SIR) during soft handoff.

4.1.1 SIR performance

The purpose of soft handoff is to improve the SIR performance for a user. Assume that a cellular system has total $|\Upsilon|$ base stations, each of which has the maximum transmission power P_{max}. According to [32], a user can apply the maximal ratio combining scheme during the soft handoff process to combine the received signals from all the base stations in the active set. Thus, the received signal for a user can be expressed as

$$SIR = \sum_{i \in \text{active set}} SIR_i = \sum_{i \in \text{active set}} \frac{S_i}{I_i + N}, \tag{4.1}$$

where SIR_i is denoted as the received SIR from base station i; S_i is the downlink received power of the serving base station i at the user terminal; N is the noise power; I_i is the sum of the inter-cell and the intra-cell interference. Specifically, SIR_i can be computed by

$$SIR_i = \frac{p_i / L_i}{\alpha \cdot P_i / L_i + \left(\sum_{j \neq i} P_j / L_j \right) + N}, \tag{4.2}$$

where p_i is the allowable transmission power allocated to a single mobile from the base station; P_i is the total transmission power of base station i ; α is the orthogonality

factor. In (5.6), L_i is defined as

$$L_i = 10^{\frac{\Omega_i}{10}} d_i^{\lambda} \ , \tag{4.3}$$

where Ω_i is the log-normally shadowing component, d_i is distance between the mobile to base station i, and λ is the path loss exponent.

Substituting (5.7) into (5.6), we obtain

$$SIR = \sum_{i \in \text{active set}} \frac{p_i / L_i}{\left(\sum_{j \in \Upsilon} \frac{P_j}{L_j} \right) + \frac{(\alpha - 1) \cdot P_i}{L_i} + N} \ , \tag{4.4}$$

where Υ is the set of all base stations in the entire system.

From (4.4) we can express the downlink SIR as follows:

$$\begin{aligned} SIR &= \sum_{j=1}^{M} \frac{p_j / L_j}{\left(\sum_{i=1}^{\Upsilon} \frac{P_{max}}{L_i} \right) + N - \frac{P_{max} \cdot (1 - \alpha)}{L_j}} \\ &= \sum_{j=1}^{M} \frac{p_j}{A L_j - B} \ , \end{aligned} \tag{4.5}$$

where M is the number of base stations in the active set,

$$A = (\sum_{i=1}^{|\Upsilon|} \frac{P_{max}}{L_i}) + N, \tag{4.6}$$

and

$$B = P_{max}(1 - \alpha) \ . \tag{4.7}$$

4.1.2 Link Proportional Power Allocation

According to the link proportional power power allocation (LPPA) method in [18], it was suggested that the transmission power of the base station during a handoff

process should be proportional to the link gain between a handover mobile to its serving base stations. To determine the transmission power based on LPPA, we have to find a set of p_i ($i = 1$ to M) such that $SIR \geq SIR_{\text{req}}$ and

$$p_1 : p_2 : \cdots : p_M = \frac{1}{L_1} : \frac{1}{L_2} : \cdots : \frac{1}{L_M} \ . \tag{4.8}$$

Subject to the constraint in (5.11), the transmission power from base station i in the active set according to the LPPA principle (denoted as $p_{i,LPPA}$) can be rewrite as

$$p_{i,LPPA} = \frac{\mathcal{P}_{LPPA}/L_i}{\frac{1}{L_1} + \frac{1}{L_2} + ... + \frac{1}{L_M}} \ , \tag{4.9}$$

where $\mathcal{P}_{LPPA}$ is the total required transmission power for the system with LPPA. Substituting (5.13) into (5.8), we have

$$\mathcal{P}_{LPPA} = \sum_{i=1}^{M} p_{i,LPPA} = \frac{SIR_{req} \cdot (\sum_{i=1}^{M} \frac{1}{L_i})}{\sum_{i=1}^{M} \frac{1/L_i}{AL_i - B}} \ , \tag{4.10}$$

where A and B are defined in (5.9) and (5.10).

4.1.3 Site Selection Diversity Transmission

In [14], the site selection diversity transmission (SSDT) technique was proposed to select the base station with the minimal path loss among the active set to serve the user. Therefore, with SSDT technique, a user is always served by the base station that transmits the least power to achieve the required performance, thereby achieving the goals of power saving and interference reduction. The SSDT scheme is viewed as a soft handoff process since it selects the best base station from the active set. As mentioned before, SSDT is viewed as the best power allocation method from the standpoint of power efficiency.

Denote p_i as the required transmission power from base station i ($i = 1$ to M) in order to maintain the required link quality for a mobile user. According to the SSDT scheme, the transmission power allocated to a target user from the selected base station with the SSDT technique (denoted by $\mathcal{P}_{SSDT}$) is expressed as

$$\begin{aligned} \mathcal{P}_{SSDT} &= p_{i,SSDT} \\ &= \min(p_1, ..., p_M) \\ &= SIR_{\text{req}} \cdot \min(AL_1 - B, .., AL_M - B) \ , \end{aligned} \tag{4.11}$$

where A and B are defined in (5.9) and (5.10).

4.1.4 Equal Power Allocation

Based on the equal power allocation (EPA) principle, all base stations involved in the handoff process will allocate the same amount of power to the target user [20]. Based on EPA, a set of p_i ($i = 1$ to M) are determined such that $SIR \geq SIR_{\text{req}}$ and

$$p_1 = p_2 = \cdots = p_M \ . \tag{4.12}$$

From (5.8), we know

$$SIR_{\text{req}} = \sum_{i=1}^{M} \frac{p_i}{AL_i - B} \ . \tag{4.13}$$

Applying the EPA constraint of (5.16) to (5.8), we obtain the transmission power from base station i in the active set is written as

$$p_{i,EPA} = \frac{SIR_{\text{req}}}{\sum_{i=1}^{M} \frac{1}{AL_i - B}} \ , \tag{4.14}$$

where A and B are defined in (5.9) and (5.10). Then, the required transmission power for a system with EPA technique (denoted by $\mathcal{P}_{EPA}$) is the sum of all the transmission

power from all the base stations in the active set. That is,

$$\mathcal{P}_{EPA} \triangleq \sum_{i=1}^{M} p_{i,EPA} = \frac{M \cdot SIR_{\text{req}}}{\sum_{i=1}^{M} \frac{1}{AL_i - B}} \quad . \tag{4.15}$$

4.1.5 Quality Balancing Power Allocation

The quality balancing power allocation (QBPA) method was introduced in [23]. The basic idea of the QBPA method is to make the received signal from all the handoff base stations be equal. Specifically, the transmission power level of the serving base stations are proportional to the path loss between the handoff user to the serving base stations. Based on QBPA, the base station transmission power, p_i ($i = 1$ to M) is determined subject to the constraints that $SIR \geq SIR_{\text{req}}$ and

$$\frac{p_1}{L_1} = \frac{p_2}{L_2} = \cdots = \frac{p_M}{L_M} \quad . \tag{4.16}$$

Applying the constraint of (5.19) to (5.8), the transmission power from base station i in the active set can be obtained as follows:

$$p_{i,QBPA} = \frac{SIR_{req} \cdot L_i}{\sum_{i=1}^{M} \frac{L_i}{AL_i - B}} \quad , \tag{4.17}$$

where A and B are defined in (5.9) and (5.10). Then by summing all the transmission power from all the base stations in the active set, the total required transmission power for a system with QBPA allocated to a mobile (denoted as $\mathcal{P}_{QBPA}$) can be computed as

$$\mathcal{P}_{QBPA} \triangleq \sum_{i=1}^{M} p_{i,QBPA} = \frac{SIR_{req} \cdot \sum_{i=1}^{M} L_i}{\sum_{i=1}^{M} \frac{L_i}{AL_i - B}} \quad . \tag{4.18}$$

4.2 Power efficiency comparison

In this section, we first analyze the power efficiency of different power allocation schemes in terms of the base station power shortage. In the literature, SSDT is shown to be the most efficient power allocation scheme by simulations. However, the property that SSDT is the most power efficient scheme has not been proved analytically. In the following, we will apply a harmonic-arithmetic mean inequality and Chebyshev-inequality to prove that SSDT is the most efficient power allocation mechanism as compared to EPA, QBPA, and LPPA mechanisms.

Lemma 1: For the same required received power at the handoff user terminal, the total required transmission power allocated from the system with the EPA method is less than or equal to that with QBPA method, i.e., $\mathcal{P}_{EPA} \leq \mathcal{P}_{QBPA}$.

Proof. From (5.18) and (5.21), we have

$$\frac{\mathcal{P}_{EPA}}{\mathcal{P}_{QBPA}} = \frac{M}{\sum_{i=1}^{M} L_i} \cdot \frac{\sum_{i=1}^{M} \frac{L_i}{AL_i - B}}{\sum_{i=1}^{M} \frac{1}{AL_i - B}} \quad , \tag{4.19}$$

where A and B are defined in (5.9) and (5.10).

Because the harmonic mean is smaller than the arithmetic mean, we can have

$$\frac{M}{\sum_{J=1}^{M} 1/L_J} \leq \frac{\sum_{J=1}^{M} L_J}{M} \quad . \tag{4.20}$$

Thus (4.19) implies that

$$\frac{\mathcal{P}_{EPA}}{\mathcal{P}_{QBPA}} \leq \frac{\sum_{i=1}^{M} 1/L_i}{M} \cdot \frac{\sum_{i=1}^{M} \frac{L_i}{AL_i - B}}{\sum_{i=1}^{M} \frac{1}{AL_i - B}}$$

$$= \frac{(\frac{1}{M}\cdot\sum_{i=a}^{M}\frac{1}{L_i})\cdot(\frac{1}{M}\cdot\sum_{i=a}^{M}\frac{L_i}{AL_i-B})}{\frac{1}{M}\cdot\sum_{i=a}^{M}\frac{1}{AL_i-B}} \ . \tag{4.21}$$

Without loss of generality, assume

$$L_1 > L_2 > ... > L_M \ . \tag{4.22}$$

Then, we have

$$\begin{cases} \frac{1}{L_1} < \frac{1}{L_2} < ... < \frac{1}{L_M} \\ \frac{L_1}{AL_1-B} < \frac{L_2}{AL_2-B} < ... < \frac{L_M}{AL_M-B} \end{cases} \tag{4.23}$$

According to the Chebyshev inequality, we know if

$$\begin{cases} 0 \le a_1 \le a_2 \le ... \le a_M \\ 0 \le b_1 \le b_2 \le ... \le b_M \end{cases} \tag{4.24}$$

then

$$(\sum_{i=1}^{M}\frac{a_i}{M})\cdot(\sum_{i=1}^{M}\frac{b_i}{M}) \le (\sum_{i=1}^{M}\frac{a_ib_i}{M}) \ . \tag{4.25}$$

Thus (4.21) leads to

$$\frac{\mathcal{P}_{EPA}}{\mathcal{P}_{QBPA}} \le \frac{(\frac{1}{M}\cdot\sum_{i=a}^{M}\frac{1}{L_i})\cdot(\frac{1}{M}\cdot\sum_{i=a}^{M}\frac{L_i}{AL_i-B})}{\frac{1}{M}\cdot\sum_{i=a}^{M}\frac{1}{AL_i-B}}$$

$$\le \frac{\frac{1}{M}\cdot\sum_{i=a}^{M}\frac{1}{AL_i-B}}{\frac{1}{M}\cdot\sum_{i=a}^{M}\frac{1}{AL_i-B}} = 1$$

$$\Rightarrow \ \mathcal{P}_{EPA} \le \mathcal{P}_{QBPA} \tag{4.26}$$

□

Lemma 2: The total required transmission power allocated from the system with the LPPA method is less than or equal to that with EPA method, i.e., $\mathcal{P}_{LPPA} \leq \mathcal{P}_{EPA}$.

Proof. From (5.14) and (5.18), we have

$$\frac{\mathcal{P}_{LPPA}}{\mathcal{P}_{EPA}} = \frac{M \cdot (\frac{1}{M}\sum_{i=1}^{M}\frac{1}{L_i})(\frac{1}{M}\sum_{i=1}^{M}\frac{1}{AL_i - B})}{\sum_{i=1}^{M}\frac{1}{L_i}\cdot\frac{1}{AL_i - B}}. \tag{4.27}$$

Similar to Lemma 1, we assume $L_1 > L_2 > ... > L_M$ and $AL_i \gg B$. From (4.23) and (4.25), we obtain

$$\begin{aligned} \frac{\mathcal{P}_{LPPA}}{\mathcal{P}_{EPA}} &\leq \frac{\sum_{J=1}^{N}\frac{1}{L_J}\cdot\frac{1}{AL_J - B}}{\sum_{J=1}^{N}\frac{1}{L_J}\cdot\frac{1}{AL_J - B}} = 1 \\ &\Rightarrow \mathcal{P}_{LPPA} \leq \mathcal{P}_{EPA} \end{aligned} \tag{4.28}$$

□

Lemma 3: The total required transmission power allocated from the system with the SSDT method is less than or equal to that with LPPA method, i.e., $\mathcal{P}_{SSDT} \leq \mathcal{P}_{LPPA}$.

Proof. From (5.15), (5.14), (4.23) and (4.25)

$$\begin{aligned}
\frac{\mathcal{P}_{SSDT}}{\mathcal{P}_{LPPA}} &= \frac{\min(AL_i - B) \cdot (\sum_{i=1}^{M} \frac{1/L_i}{AL_i - B})}{\sum_{i=1}^{M} \frac{1}{L_i}} \\
&\leq \frac{\sum_{J=1}^{N} \frac{1/L_J}{AL_J - B} \cdot AL_J - B}{\sum_{J=1}^{N} \frac{1}{L_J}} = 1 \\
&\Rightarrow \mathcal{P}_{SSDT} \leq \mathcal{P}_{LPPA} \qquad (4.29)
\end{aligned}$$

□

Theorem 1: The total required transmission power required for the system with the QBPA, EPA, LPPA, and SSDT methods are listed from the least power efficient to the most power efficient, i.e., $\mathcal{P}_{SSDT} \leq \mathcal{P}_{LPPA} \leq \mathcal{P}_{EPA} \leq \mathcal{P}_{QBPA}$.

Proof. Theorem 1 is proved by observing Lemmas 1, 2, and 3. □

To summarize, different power allocation schemes lead to different total transmission power allocated from the system. The less the power required, the higher will be the power efficiency. From Theorem 1, we conclude that SSDT is the most efficient power allocation scheme, while QBPA is the worst one.

4.3 Power Control Error Sensitivity

Besides base station power shortage, the power control error is another factor causing performance outage. In this section, we will derive closed-form expressions for outage

probability of downlink power allocation mechanisms due to power control errors. The outage probability is defined as

$$P_{out} = \text{Prob}(SIR < SIR_{threshold}), \tag{4.30}$$

where

$$SIR_{threshold} = SIR_{target} \cdot 10^{\kappa/10},$$

and κ is the SIR outage margin in the dB domain. For notation simplification, let $I_i = A - B/L_j$. From (5.8), the target SIR can be written as

$$SIR_{target} = \sum_{i=1}^{M} \frac{p_i/L_i}{I_i} = \sum_{i=1}^{M} \frac{p_i}{L_i \cdot I_i}, \tag{4.31}$$

where p_i is the transmission power of base station i serving a specific mobile with perfect power control, and I_i is the corresponding interference. Let a power control error (denoted as χ_i) be modelled by a Gaussian random variable with zero mean and a standard deviation of σ_χ [20]. The received SIR can be expressed as

$$SIR = \sum_{i=1}^{M} \frac{p_i/L_i \cdot 10^{\chi_i/10}}{I_i} = \sum_{i=1}^{M} \frac{p_i \cdot 10^{\chi_i/10}}{L_i \cdot I_i}. \tag{4.32}$$

Then, we have

$$\begin{aligned} P_{out} &= \text{Prob}\left(\frac{\sum_{i=1}^{M} \frac{p_i \cdot 10^{\chi_i/10}}{L_i \cdot I_i}}{\sum_{j=1}^{M} \frac{p_j}{L_j \cdot I_j}} < 10^{-\kappa/10}\right) \\ &= \text{Prob}\left(\sum_{i=1}^{M} e^{\zeta_i} < 10^{-\kappa/10}\right), \end{aligned} \tag{4.33}$$

where ζ_i is a Gaussian random variable with mean

$$\mu_{\zeta_i} = \ln 10 \cdot \log\left(\frac{\frac{p_i}{L_i \cdot I_i}}{\sum_{j=1}^{M} \frac{p_j}{L_j \cdot I_j}}\right), \tag{4.34}$$

and standard deviation

$$\sigma_{\zeta_i} = \frac{\ln 10}{10} \cdot \sigma_\chi. \tag{4.35}$$

By using the Fenton-Wilkinson's approximation [36], we approximate the sum of log-normal random variables as another log-normal random variable ψ. That is

$$e^\psi = \sum_{i=1}^{M} e^{\zeta_i}, \tag{4.36}$$

where the mean of ψ is

$$\mu_\psi = 2\ln(u_1) - \frac{1}{2}\ln(u_2), \tag{4.37}$$

and its variance is

$$\sigma_\psi^2 = 2\ln(u_2) - 2\ln(u_1). \tag{4.38}$$

Note that in (5.49) and (5.50),

$$u_1 = \sum_{i=1}^{M} e^{\mu_{\zeta_i} + \sigma_{\zeta_i}^2/2} \tag{4.39}$$

and

$$\begin{aligned} u_2 \;=\; & \sum_{i=1}^{M} e^{2\mu_{\zeta_i} + 2\sigma_{\zeta_i}^2} \\ & + 2\sum_{i=1}^{M-1}\sum_{j=i+1}^{M} \{e^{\mu_{\zeta_i} + \mu_{\zeta_j}} \cdot e^{\frac{1}{2}(\sigma_{\zeta_i}^2 + \sigma_{\zeta_j}^2 + 2r_{ij}\sigma_{\zeta_i}\sigma_{\zeta_j})}\}. \end{aligned} \tag{4.40}$$

Then (4.33) can be simplified as

$$\text{Prob}(\sum_{i=1}^{M} e^{\zeta_i} < 10^{-\kappa/10}) = \text{Q}(\frac{\frac{\ln 10}{10}\kappa + \mu_\psi}{\sigma_\psi}) \ , \tag{4.41}$$

where

$$\text{Q}(x) = \frac{1}{\sqrt{2\pi}} \int_x^\infty e^{-\frac{t^2}{2}} dt \ . \tag{4.42}$$

Note that μ_ψ and σ_ψ are functions of p_i depending on different power allocation schemes from (4.34) to (5.52). Combining (5.13) and (5.14), we can obtain p_i under LPPA as

$$p_{i,LPPA} = \frac{SIR_{target} \cdot \frac{1}{L_i}}{\sum_{l=1}^{M} \frac{\frac{1}{L_l}}{A \cdot L_l - B}}. \tag{4.43}$$

By substituting $p_{i,LPPA}$ of (4.43) into p_i in (4.34) and (4.41), we can obtain the outage probability with LPPA subject to power control error.

Similarly, by substituting $p_{i,SSDT}$, $p_{i,EPA}$ and $p_{i,QBPA}$ obtained from (5.15), (5.17) and (5.20) into p_i of (4.34) and (4.41), we can obtain the corresponding outage probability due to power control errors for power allocation mechanisms SSDT, EPA, and QBPA, respectively. From (4.34) to (4.43), one can see that the outage probability due to power control errors is related to of L_i and A, both which are functions of the distance between a mobile and base stations according to (4.3) and (5.9). Therefore, the outage probability due to power control errors is dependent on both the mobile locations and power allocation schemes.

4.4 Numerical Results

In this section, we provide the simulation and analytical results for four power allocation schemes. Both the effects of base station power shortage and power control errors are considered. We first compare the power efficiency and the sensitivity to power control errors for different power allocation schemes. Then we show the impacts of both outage factors on the performance of downlink power allocation mechanisms.

4.4.1 Simulation Environment

We apply a wrap around technique to simulate a cellular system with 19 cells as shown in Figure 1. Refer to [32], the environment parameters used in simulation are listed in Table I. We assume that all the mobiles are uniformly distributed in the system. Each mobile moves at the speed of 80 km/hr with probability of changing direction equal to 0.2, and the range of turning angle is 45 degrees.

4.4.2 Results of Power Efficiency

In Section 4.2, our analysis has shown that SSDT has the best power efficiency, while QBPA performs worst. Figure 2 shows the simulation result of outage probability with different system loads and different power allocation algorithms. As shown in the figure, SSDT has the lowest outage probability under different system loads. In this example, if the required outage probability is 10 %, the system capacity with SSDT, LPPA, EPA, and QBPA are 46, 41, 35, and 23, respectively. This simulation result verifies Theorem 1 in Section 4.2.

4.4.3 Effects of Power Control Errors

Now we present the outage probability performance of power allocation mechanisms due to power control errors. We investigate the behavior of one mobile moving from base station 1 to base station 2 along with a straight line. We compare the outage probability purely caused by power control errors for LPPA, EPA, QBPA and SSDT. Let the SIR margin κ be 1, power control error factor σ_χ be 0.5, and handoff threshold be 5 dB. Figure 3 shows the impact of power control errors on the power allocation mechanisms in terms by evaluating (4.41). One can observe that QBPA is the least sensitive to power control errors, while SSDT is the most sensitive to power control errors. The outage probability differences due to power control errors for four power

allocation schemes can be as high as 5.9 % percent at the normalized distance equal to one.

4.4.4 Effect of Both Power Efficiency and Power Control Error

So far we have shown the outage probability due to base station power shortage and power control errors in Fig. 2 and Fig. 3, respectively. Now we want to combine these two outage factors together.

$$\begin{aligned} \text{Prob}(\textit{outage}) &= \text{Prob(BS power shortage)} + [1 - \text{Prob(BS power shortage)}] \\ &\quad \cdot \text{Prob(outage due to power control errors)} \ . \end{aligned} \tag{4.44}$$

Because the simulated outage performance of base station power shortage outage is combined with analytical outage due to power control errors, this is a semi-analytical approach. In this simulation, all the mobiles are uniformly distributed in the system and the soft handoff threshold is set to be 5 dB. The sensitivity to power control errors differs most at the normalized distance equal to one, so we first show the performance of one fixed point at normalized distance equal to one.

First, we use a special case to verify our analytical result by simulation. Figure 4 shows the outage probability of a particular mobile located at the cell boundary when applying the SSDT and LPPA mechanisms with base station power constraints and power control errors, where the SIR margin κ is 1, power control error factor σ_χ is 0.5, handoff threshold is 5 dB, and the other system parameters are listed in Table 1. The pure simulation results in the figure match our semi-analytical results. From the figure, we find that when the average number of users in a base station is less than 40, SSDT exhibits higher outage probability, while LPPA is the better choice. This observation implies that the advantage of SSDT on power efficiency is not sufficient

enough to offset the degradation of the sensitivity to power control errors in a typical system load.

Now, we provide a more general numerical result. Figure 5 shows the comparison of average outage probability for all the handoff users applying four power allocation mechanisms with the total power constraint and power control errors, where the handoff threshold is 5 dB as the previous case. We find that QBPA leads to the lowest outage probability under the light system load. When there are 15 users per cell, the outage probability of SSDT, LPPA, EPA, and QBPA are 7.5, 5, 4, and 2.5 percent, respectively. However, the system performances of four power allocation schemes change as the system load increases. If the maximum outage probability accepted is 9 %, the system capacity with SSDT, LPPA, EPA, and QBPA are 38, 38, 33, and 22, respectively. Note that LPPA approaches the maximum system capacity when the outage probability is set to be less than 9 %. Nevertheless, SSDT outperforms other power allocation schemes only with the heavy load situation, i.e., the number of users is larger than 38 per cell. In this heavy load case, the outage performance is as high as 9 %, which may not be practical in some situations.

4.4.5 Discussion

Each power allocation scheme has different pros and cons as seen in Fig. 5. However, it is hard to say which one is the best power allocation strategy, because it depends on the angle of comparing different power allocation schemes. For example, SSDT achieves the highest system capacity if the maximum acceptable outage probability is set to be 10 %. Nevertheless, the system with SSDT suffers a higher outage probability when the system load is not so heavy, e.g., less than 37 mobiles in a cell. Furthermore, QBPA provides the lowest outage probability when the number of mobiles in a cell is less than 17, but QBPA system can only support 22 mobiles per

cell, which is the lowest for the required outage probability is lower than 10 %. Note that EPA exhibits slightly higher outage probability under light system load, but has much higher capacity than QBPA. Interestingly, LPPA approaches almost the same capacity as SSDT, while maintaining lower outage probability than SSDT. According to above discussions, LPPA seems to be a better choice because it can achieve high capacity. However, LPPA may requires more computations and signaling traffic.

4.5 Conclusions

In this chapter, we have investigated the performance of different downlink power allocation schemes for soft handoff in CDMA systems subject to power control errors. With consideration of both base station power shortage and power control errors, we analyze the outage and capacity performances of equal power allocation (EPA), quality balancing power allocation (QBPA), site selection diversity transmission (SSDT), and link proportional power allocation (LPPA) mechanisms.

Our numerical results demonstrate that due to power control errors the SSDT system suffers from a higher outage probability in the moderate traffic load condition although it can achieve the best outage probability performance in the heavy traffic condition. Furthermore, we show that the LPPA system can almost approach the capacity of the SSDT system, while maintaining lower outage probability than SSDT in the moderate traffic.

Some interesting research topics extended from this work include the selection of optimal handoff parameters, and the impact of correlated shadowing and Rician factor on the downlink power allocation schemes.

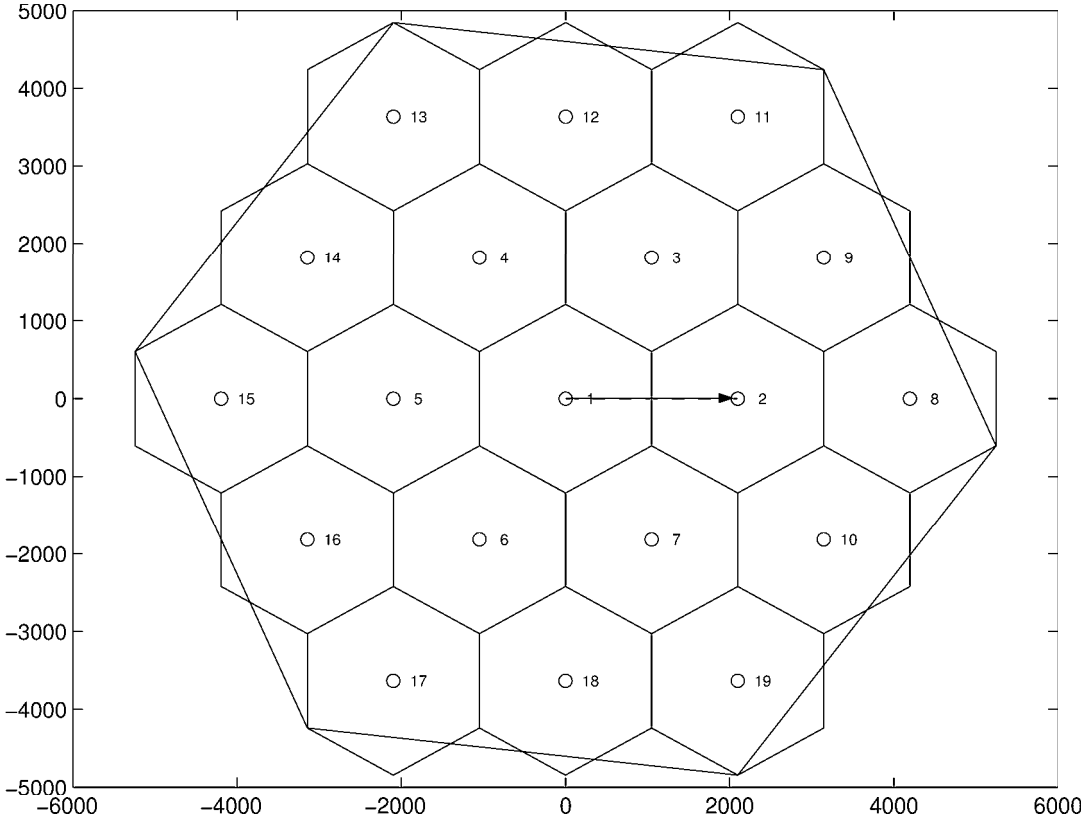

Figure 4.1: Base station layout in simulations.

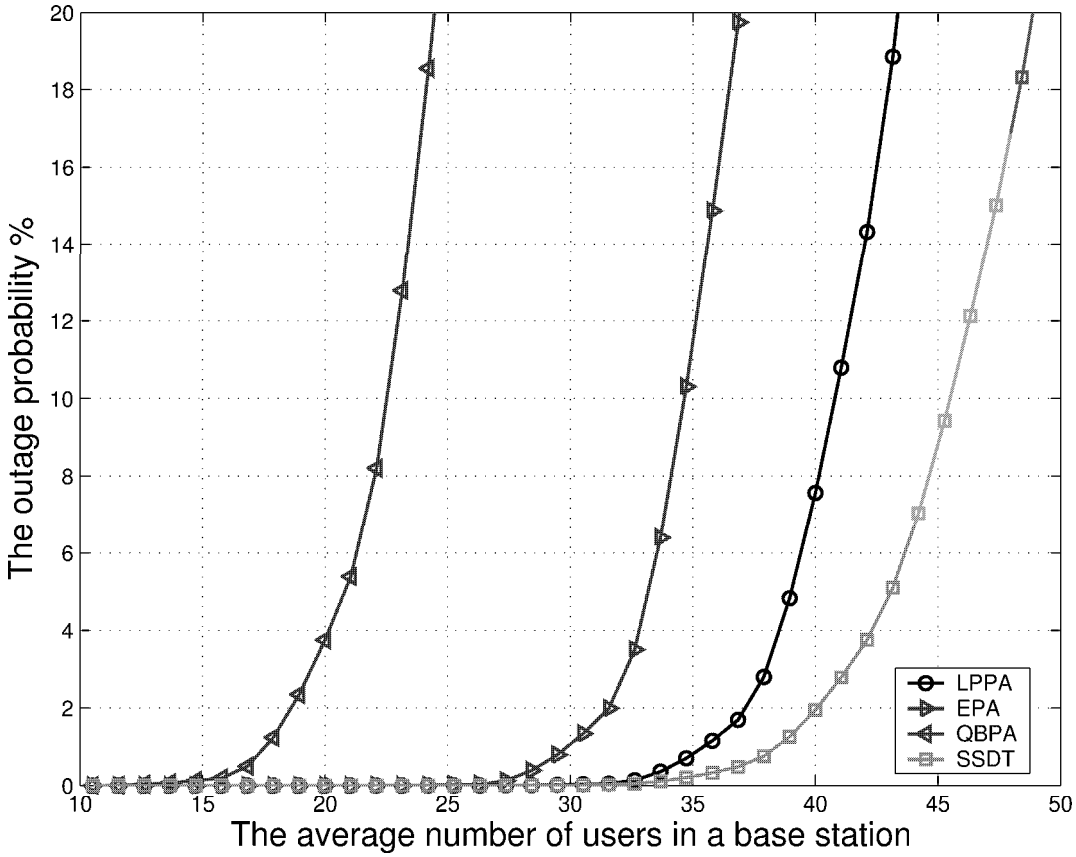

Figure 4.2: Outage probability comparison of four power allocation mechanisms with total power constrain and without power control error. This simulation is under environment with system parameters listed in Table 1.

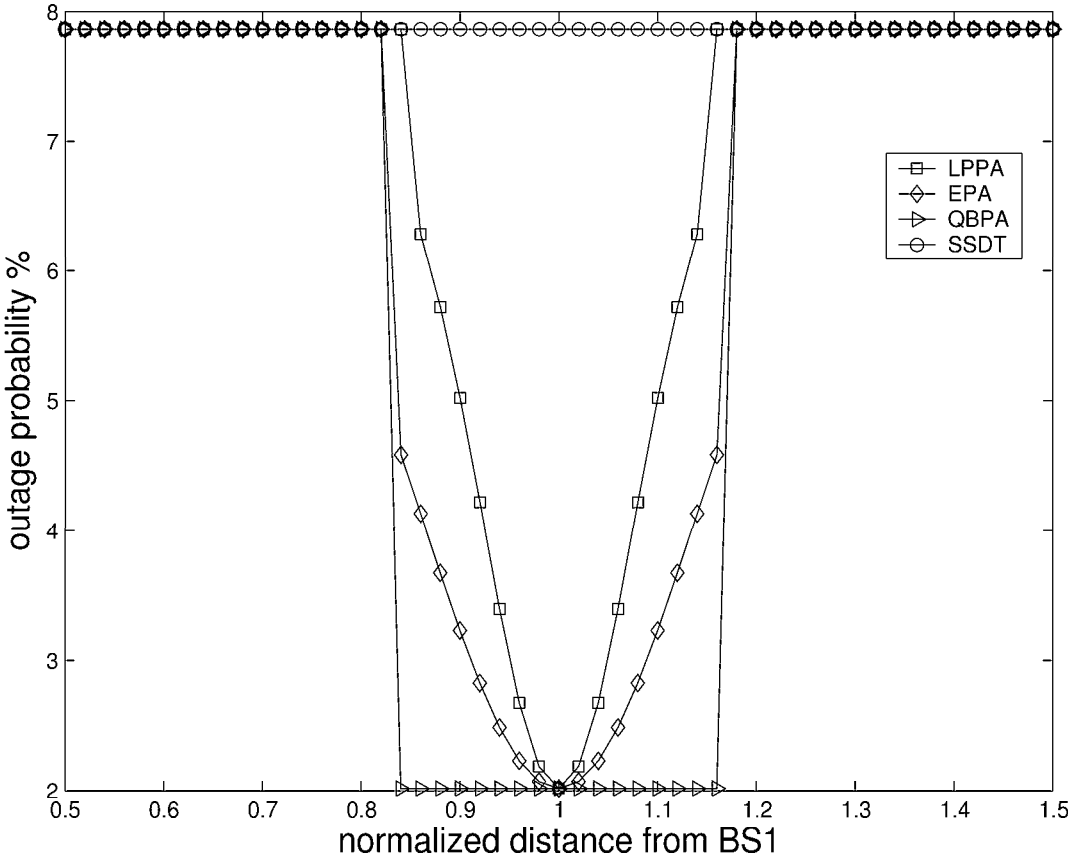

Figure 4.3: Sensitivity of power allocation mechanisms to power control error without the total power constraint. This simulation is under environment with system parameters listed in Table 1 while letting the SIR margin κ be 1, power control error factor σ_χ be 0.5, and handoff threshold be 5 dB.

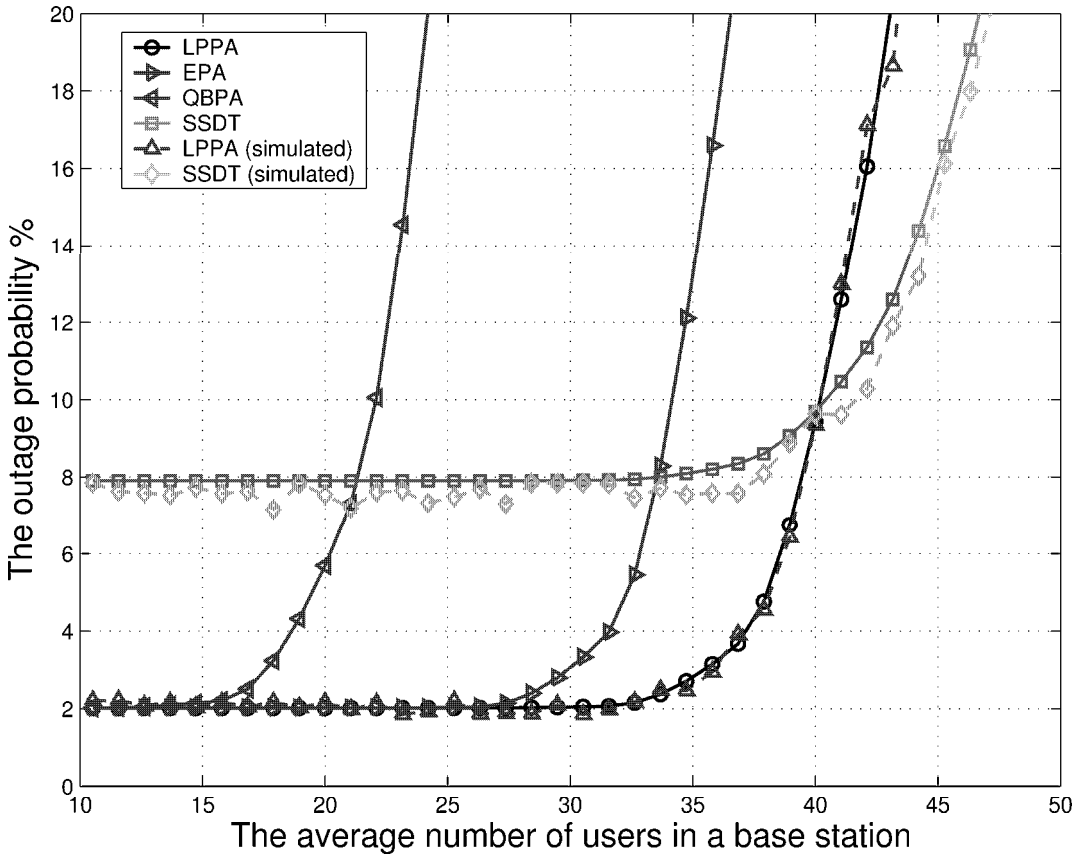

Figure 4.4: Outage probability of a particular mobile located at the cell boundary when applying the SSDT and LPPA schemes. The pure simulation results are also provided to verified our analytical results, where the SIR margin κ is 1, power control error factor σ_χ is 0.5, and handoff threshold is 5 dB, and the other system parameters are listed in Table 1.

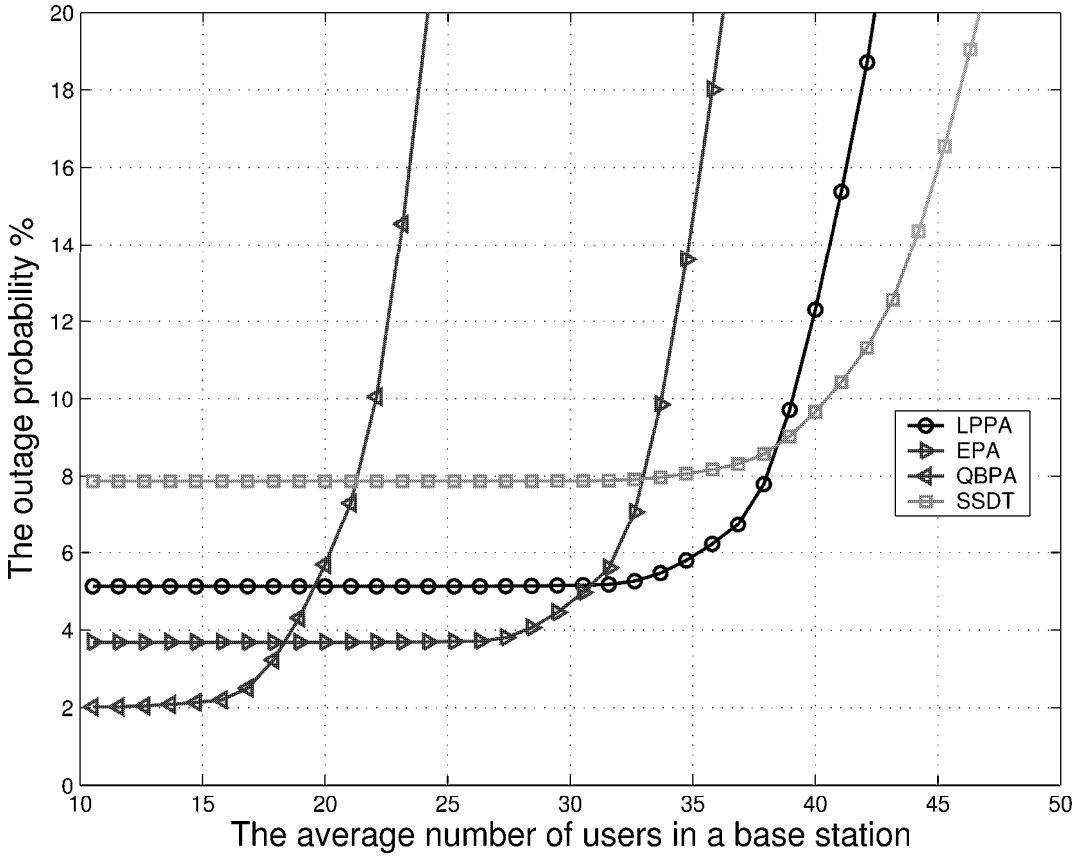

Figure 4.5: Comparison of average outage probability for all the handoff users applying four power allocation mechanisms with the total power constraint and power control errors, where the SIR margin κ is 1, power control error factor σ_χ is 0.5, and handoff threshold is 5 dB.

Table 4.1: Simulation Parameters

the total number of cells, Υ	19
antenna type	omni-directional
radius	1211 m
max. base station tran. power, $P_{\max}$	30 dBm
processing gain	24.9 dB
the required signal quality, E_b/N_o	7.9 dB
de-correlation distance, d_{dec}	20 m
shadowing standard deviation, σ	10 dB
handoff threshold	5 dB
orthogonality factor, α	0.5
noise power, N	-99 dBm

CHAPTER 5

Performance Analysis of Downlink Power Allocation Mechanisms for Soft Handoff in the WCDMA System with Co-channel Interference

The growing demands for the mobile multimedia services have posed a new challenge on the next generation wireless systems. On of the key challenges is to provide seamless handoff for a high-speed mobile transmitting high-volume real-time multimedia traffic.

Soft handoff has been viewed as an inevitable technique of the code division multiple access (CDMA) system to maintain the radio link quality for a user terminal moving across the cell boundary since the introduction of the second generation cellular mobile systems. The conventional soft handoff mechanisms are effective in the 2^{nd} generation voice-oriented cellular mobile networks, and the soft handoff issue has been investigated for ten years [12,33,34]. Nevertheless, it is still a hot research area to improve the soft handoff mechanisms for supporting high data-rate real-time services, especially in the downlink.

To support high volume downlink transmission for soft handoff users, various downlink power allocation mechanisms have been proposed in the literature [14,15,

17–23]. The key challenges in designing downlink power allocation mechanisms lie in two folds. First, power efficiency of the power allocation mechanisms is required to be carefully evaluated because each wireless Internet user demands more power to support its high data rate services. Second, outage performance subject to co-channel interference becomes a critical issue since the link quality is the key requirement for the wireless multimedia service. To our knowledge, an analytical evaluation on the power efficiency and the outage probability subject to co-channel interference of different power allocation mechanisms in soft handoff is still lacking in the literature.

The prior studies on the downlink power allocation mechanism for soft handoff can be summarized as follows. Four different downlink power allocation mechanisms have been reported in the literature, including the site selection diversity transmission (SSDT) [14] [15], the link proportional power allocation (LPPA) [17–19], the equal power allocation (EPA) [20–22], and the quality balancing power allocation (QBPA) [23]. The SSDT mechanism was shown to be most power efficient downlink power allocation scheme by simulations in [23] and by proof in [19], respectively. However, in [19], the exact amount of consumed power was still obtained by simulations. The impact of power control errors on the power allocation mechanisms was investigated in [35]. Recently, in [37], the authors analyzed the outage performance of the EPA-based soft handoff in the Rayleigh fading channel. However, the power efficiency of the considered soft handoff algorithm and the impact of co-channel interference were not considered in [37].

This chapter includes two major objectives. The first goal of this chapter is to develop an analytical approach to evaluate the power efficiency of different power allocation mechanisms in soft handoff. The second goal of this work is to present an analytical expression for evaluating the outage probability of a soft handoff user when applying different power allocation mechanisms in the lognormally-shadowed Rician fading channel subject to multiple lognormally-shadowed Rayleigh fading co-channel

interferences. We will apply the developed analytical methods to explicitly estimate the consumed power for different power allocation mechanisms and evaluate the effects of soft handoff threshold, orthogonality factor of the channelization codes, and the Rician fading K factor on the outage performance of the soft handoff algorithms subject to co-channel interference.

The rest of this paper is organized as follows. Section 5.1 describes radio channel, SIR performance model. Section 5.2 illustrates the four considered power allocation schemes, i.e. SSDT, LPPA, EPA, QBPA. Section 5.3 analyzes the power efficiency of the four power allocation schemes. Section 5.4develops the analytical model for evaluating the outage probability of soft handoff algorithm in the log-normally shadowed Rician fading channel subject to co-channel interference. Section 5.5 gives some numerical results. We give our concluding remarks in Section 5.6.

5.1 Radio Channel and SIR Performance Models

In this chapter, we consider a radio channel model characterized by path loss, log-normally shadowing and Rician fast fading.

5.1.1 Path Loss and Shadowing

To begin with, the joint path loss with log-normally distributed shadowing in decibels is characterized by a multivariate Gaussian variable, i.e.

$$\boldsymbol{L} = \begin{bmatrix} L_1 \\ \vdots \\ L_\Upsilon \end{bmatrix} \sim \mathcal{N}\left(\begin{bmatrix} 10\delta \log(d_1) \\ \vdots \\ 10\delta \log(d_\Upsilon) \end{bmatrix}, \sigma^2 \mathbf{C} \right), \tag{5.1}$$

where Υ is the total number of base stations in the system, δ is the path loss exponent, d_i is the distance between a mobile and base station i, σ^2 is the variance of the log-

normal shadowing. In (5.1), $\mathbf{C} = [c_{i,j}]_{i,j=1}^{\Upsilon}$, and $c_{i,j}$ is the path loss correlation between base stations i and j, defined as

$$c_{i,j} = a + b\cos\theta_{i,j} \ , \tag{5.2}$$

where $\theta_{i,j}$ is the subtending angle of base stations i and j to the mobile and $\{a, b\}$ are tunable parameters.

5.1.2 Rician Fading

In the propagation model with a line-of-sight (LOS) or specular component, the instantaneous received signal amplitude (denoted as x_d) is Rician distributed. If the scattered power of the received signal is σ_d^2 and the amplitude of the dominant component is A_d, then the probability densiti function (pdf) of the instantaneous received signal is

$$f_{x_d}(x_d|\sigma_d^2, A_d) = \frac{x_d}{\sigma_d^2}\exp[\frac{-(x_d^2 + A_d^2)}{2\sigma_d^2}]I_0(\frac{A_d x_d}{\sigma_d^2}) \ , \tag{5.3}$$

where I_0 is the zeroth order modified Bessel function of the first kind. Then the instantaneous received signal power (denoted as $s_d = x_d^2/2$) conditioned on the local mean power (denoted as $\Omega_d = A_d^2/2\sigma_d^2$) has the non-central chi-square distribution

$$f_{s_d|\Omega_d}(s_d|\Omega_d) = \frac{K_d + 1}{\Omega_d}\exp[-K_d - \frac{(K_d+1)s_d}{\Omega_d}]I_0\left(\sqrt{\frac{4K_d(K_d+1)s_d}{\Omega_d}}\right) \ , \tag{5.4}$$

where Rice factor $K_d = A_d^2/2\sigma_d^2$ is defined as the ratio of the direct power to the scattered power.

5.1.3 SIR Performance

The purpose of soft handoff is to improve the signal-to-interference ratio (SIR). Here, we discuss how to calculate SIR during soft handoff. Assume that each base station

has the maximum transmission power P_{max} and define $f = |M|$ as the number of base stations in the active set for a particular user. Specifically, the active set is defined as

$$\begin{aligned} M &= \left\{ i | 1 \le i \le \Upsilon, 10\log\frac{P_{pilot}}{10^{\frac{L_i}{10}}} \ge 10\log\left(\max_{1\le j\le\Upsilon}\frac{P_{pilot}}{10^{\frac{L_j}{10}}}\right) - \tau \right\} \\ &= \left\{ i | 1 \le i \le \Upsilon, L_i \ge \max_{1\le j\le\Upsilon} L_j - \tau \right\} \ , \end{aligned} \tag{5.5}$$

where P_{pilot} is the pilot signal power and τ is soft handoff threshold. According to [32], a user can apply the maximal ratio combining scheme during soft handoff to combine the received signals from all the base stations in the active set. Thus, the received signal for a handoff user can be expressed as

$$SIR = \sum_{i\in \mathrm{M}} SIR_i = \sum_{i\in \mathrm{M}} \frac{S_i}{I_i + N} \ , \tag{5.6}$$

where SIR_i is denoted as the received SIR from base station i; S_i is the downlink received power of the serving base station i at the user terminal; N is the noise power; I_i is the sum of the inter-cell and the intra-cell interference. Specifically, SIR_i can be computed by

$$SIR_i = \frac{p_i/L_i}{\alpha \cdot P_i/L_i + \left(\sum_{j\neq i} P_j/L_j\right) + N} \ , \tag{5.7}$$

where p_i is the allowable transmission power allocated to a single mobile from the base station i; P_i is the total transmission power of base station i ; α is the orthogonality factor.

Substituting (5.7) into (5.6), we obtain

$$\begin{aligned} SIR &= \sum_{i\in \mathrm{M}} \frac{p_i/L_i}{\left(\sum_{j\in\Upsilon}\frac{P_j}{L_j}\right) + \frac{(\alpha-1)\cdot P_i}{L_i} + N} \\ &= \sum_{j=1}^{M} \frac{p_j}{AL_j - B} \ , \end{aligned} \tag{5.8}$$

where

$$A = (\sum_{i=1}^{|\Upsilon|} \frac{P_i}{L_i}) + N, \tag{5.9}$$

and

$$B = P_i(1-\alpha) \ . \tag{5.10}$$

5.2 Downlink Power Allocation Mechanisms

A downlink soft handoff process requires multiple base stations to simultaneously allocate power to a mobile terminal during handoff. There are four downlink power allocation strategies considered in this chapter, including (1) link proportional power allocation (LPPA), (2) site selection diversity transmission (SSDT), (3) equal power allocation (EPA), and (4) quality balancing power allocation (QBPA).

5.2.1 Link Proportional Power Allocation

According to the link proportional power power allocation (LPPA) method in [18], the transmission power of the base station during a handoff process should be proportional to the link gain between a handover mobile to its serving base stations. To determine the transmission power based on LPPA, we have to find a set of p_i ($i = 1$ to f) such that

$$p_1 : p_2 : \cdots : p_f = \frac{1}{L_1} : \frac{1}{L_2} : \cdots : \frac{1}{L_f} \ , \tag{5.11}$$

and

$$SIR \geq SIR_{\text{req}} \ , \tag{5.12}$$

where SIR_{req} is the received target SIR.

Then, the transmission power from base station i in the active set is

$$p_{i,LPPA} = \frac{SIR_{req}}{L_i \sum_{j=1}^{f} \frac{1/L_j}{AL_j - B}} \ , \tag{5.13}$$

Substituting (5.13) into (5.8), the total required transmission power for the system with LPPA (denoted by $\mathcal{P}_{LPPA}$) allocated a particular user is equal to

$$\mathcal{P}_{LPPA} = \sum_{i=1}^{f} p_{i,LPPA} = \frac{SIR_{req} \cdot (\sum_{i=1}^{f} \frac{1}{L_i})}{\sum_{i=1}^{f} \frac{1/L_i}{AL_i - B}} \ , \tag{5.14}$$

where A and B are defined in (5.9) and (5.10).

5.2.2 Site Selection Diversity Transmission

In [14], the site selection diversity transmission (SSDT) technique was proposed to select the base station with the minimal path loss among the active set to serve the user. Therefore, a user in the system applying the SSDT technique can be always served by the base station requiring the least transmission power to achieve the required SIR performance, thereby achieving the goals of power saving and interference reduction. The SSDT scheme is viewed as a soft handoff process since it dynamically maintains an active set of better serving base stations. As mentioned before, SSDT is viewed as the best power allocation method from the standpoint of power efficiency.

Denote p_i as the required transmission power from base station i in order to maintain the required link quality for a mobile user, where $i = 1$ to f. According to the SSDT scheme, the transmission power allocated to a target user from the selected base station with the SSDT technique (denoted by $\mathcal{P}_{SSDT}$) is expressed as

$$\begin{aligned} \mathcal{P}_{SSDT} &= p_{i,SSDT} \\ &= \min(p_1, ..., p_f) \\ &= SIR_{\text{req}} \cdot \min(AL_1 - B, .., AL_f - B) \ , \end{aligned} \tag{5.15}$$

where A and B are defined in (5.9) and (5.10).

5.2.3 Equal Power Allocation

Based on the equal power allocation (EPA) principle, all base stations in the active set will allocate the same amount of power to the target user [20]. Based on this principle, a set of p_i ($i = 1$ to f) are needed to be determined such that $SIR \geq SIR_{\text{req}}$ and

$$p_1 = p_2 = \cdots = p_f \ . \tag{5.16}$$

Applying the EPA constraint of (5.16) to (5.8), we obtain the transmission power from base station i in the active set is

$$p_{i,EPA} = \frac{SIR_{\text{req}}}{\sum_{i=1}^{f} \frac{1}{AL_i - B}} \ , \tag{5.17}$$

where A and B are defined in (5.9) and (5.10). Then, the required transmission power for a system with EPA technique (denoted by $\mathcal{P}_{EPA}$) is the sum of all the transmission power from all the base stations in the active set. That is,

$$\mathcal{P}_{EPA} \triangleq \sum_{i=1}^{f} p_{i,EPA} = \frac{f \cdot SIR_{\text{req}}}{\sum_{i=1}^{f} \frac{1}{AL_i - B}} \ . \tag{5.18}$$

5.2.4 Quality Balancing Power Allocation

The quality balancing power allocation (QBPA) method was introduced in [23]. The basic idea of the QBPA method is to equalize the received signal from all the handoff base stations. More specifically, the transmission power level of the serving base stations are proportional to the path loss between the handoff user to the serving base stations. Based on QBPA, the base station transmission power, p_i ($i = 1$ to f) is determined subject to the condition that $SIR \geq SIR_{\text{req}}$ and

$$\frac{p_1}{L_1} = \frac{p_2}{L_2} = \cdots = \frac{p_f}{L_f} \ . \tag{5.19}$$

Applying the constraint of (5.19) to (5.8), the transmission power from base station i in the active set can be obtained as follows:

$$p_{i,QBPA} = \frac{SIR_{req} \cdot L_i}{\sum_{i=1}^{f} \frac{L_i}{AL_i - B}} \quad , \tag{5.20}$$

where A and B are defined in (5.9) and (5.10). By summing all the transmission power from all the base stations in the active set, the total required transmission power for following the QBPA priciple (denoted as $\mathcal{P}_{QBPA}$) can be computed as

$$\mathcal{P}_{QBPA} \triangleq \sum_{i=1}^{f} p_{i,QBPA} = \frac{SIR_{req} \cdot \sum_{i=1}^{f} L_i}{\sum_{i=1}^{f} \frac{L_i}{AL_i - B}} \quad . \tag{5.21}$$

5.3 Power Efficiency Analysis

Power efficiency is an important performance measure to evaluation power allocation schemes. The power efficiency will be directly related to the system capacity due to the limitation of the total transmission power at a base station. The power efficiency of the four aforementioned power allocation schemes has been compared relatively in [35]. However, the exact consumed power of each power allocation scheme was obtained only by simulation in [35]. Thus, we aim to develop an analytical method to calculate the power efficiency performance.

In the following, we utilize the concept of active set distribution in [37] to calculate the consumed power when applying different power allocation schemes. Denote the path loss of the dominant base station k as L_k. Here, the dominant base station represents the base station with the smallest path loss. Next, we define the path loss

difference matrix as

$$\boldsymbol{V}_k \triangleq \begin{bmatrix} L_1 - L_k \\ \vdots \\ L_{k-1} - L_k \\ L_{k+1} - L_k \\ \vdots \\ L_\Upsilon - L_k \end{bmatrix} \sim \mathcal{N}(\mathbf{U}_k, \sigma^2 \widehat{\mathbf{C}}_k) \ , \tag{5.22}$$

where

$$\mathbf{U}_k = \begin{bmatrix} 10\delta \log(d_1) - 10\delta \log(d_k) \\ \vdots \\ 10\delta \log(d_{k-1}) - 10\delta \log(d_k) \\ 10\delta \log(d_{k+1}) - 10\delta \log(d_k) \\ \vdots \\ 10\delta \log(d_\Upsilon) - 10\delta \log(d_k) \end{bmatrix} . \tag{5.23}$$

Note that

$$\widehat{\mathbf{C}}_k = [\widehat{c}_{k,m,n}]_{m,n=1}^{\Upsilon-1} \ , \widehat{c}_{k,m,n} = 1 - c_{k,n} - c_{k,m} + c_{m,n} \ , \tag{5.24}$$

where $c_{i,j}$ is defined in (5.2).

Assume that base station k is the dominant base station in the active set M. Then, it is possible to have $H_{k,f}$ different combinations of active set, i.e.

$$H_{k,f} = \begin{pmatrix} \Upsilon - 1 \\ f - 1 \end{pmatrix} . \tag{5.25}$$

Denote $\boldsymbol{V}_{k,f,w}$ as the corresponding path loss difference matrix for the q^{th} combination out of $H_{k,f}$. For the expression notation's simplification, we use a permutation matrix $\boldsymbol{P}_{k,f,q}$ to move the path loss difference elements of base stations in the active set to

the first $f-1$ elements of a new matrix $\boldsymbol{V}'_{k,f,q}$. We define the permutation matrix as

$$\boldsymbol{P}_{k,f,q} = [\widetilde{p}_{i,j}]_{i,j=1}^{|\Upsilon|-1} \ , \ \widetilde{p}_{i,j} = \begin{cases} 1 \ , \ \text{if} & i = z \ \text{and} \ j = m_z \ ; \\ & i = z+f-1 \ \text{and} \ j = \widehat{m}_z \\ 0 \ , \ \text{else} \end{cases} , \tag{5.26}$$

where m_z is the z^{th} element of active set $M_{k,f,q}$ except the index of the dominant base station k, and $\widehat{m}_z$ is the z^{th} element of the complemental set (denoted by $\widehat{M}_{k,f,q}$) of active set.

The matrix after the process of rearrangement becomes

$$\boldsymbol{V}'_{k,f,q} = \begin{bmatrix} v'_{k,f,q,1} \\ \vdots \\ v'_{k,f,q,\Upsilon-1} \end{bmatrix} = \boldsymbol{P}_{k,f,q}\boldsymbol{V}_{k,f,q} \sim \mathcal{N}\left(\boldsymbol{P}_{k,f,q}\mathbf{U}_k, \sigma^2\boldsymbol{P}_{k,f,q}\widehat{\mathbf{C}}_k\boldsymbol{P}_{k,f,q}^T\right). \tag{5.27}$$

The corresponding base stations of $v'_{k,f,q,1}\ldots v'_{k,f,q,f-1}$ and base station k are in the active set. The probability that $\boldsymbol{V}'_{k,f,q}$ occurs is equal to the probability of $\boldsymbol{M}_{k,f,q}$. Specifically,

$$\begin{aligned} & Pro\{\boldsymbol{V}'_{k,f,q}\} = Pro\{\boldsymbol{M}_{k,f,q}\} \\ = & \int_{(0,\tau]^{f-1}} dv'_{k,f,q,1}\ldots dv'_{k,f,q,f-1} \int_{(\tau,\infty)^{\Upsilon-f}} dv'_{k,f,q,f}\ldots dv'_{k,f,q,\Upsilon-1} \\ & \frac{\exp\left\{-[\boldsymbol{V}'_{k,f,q}-\boldsymbol{P}_{k,f,q}\mathbf{U}_k]^T\boldsymbol{P}_{k,f,q}^{-T}\mathbf{C}_k^{-1}\boldsymbol{P}_{k,f,q}^{-1}[\boldsymbol{V}'_{k,f,q}-\boldsymbol{P}_{k,f,q}\mathbf{U}_k]/(2\sigma^2)\right\}}{\sqrt{(2\pi\sigma^2)^{\Upsilon-1}\det[\boldsymbol{P}_{k,f,q}\widehat{\mathbf{C}}_k\boldsymbol{P}_{k,f,q}^T]}}. \end{aligned} \tag{5.28}$$

Note that the summation of probability of all possible $\boldsymbol{M}_{k,f,q}$ should be equal to 1, i.e.

$$\sum_{k=1}^{\Upsilon}\sum_{f=1}^{\Upsilon}\sum_{q=1}^{H_{k,f}} Pro\{\boldsymbol{M}_{k,f,q}\} = 1. \tag{5.29}$$

Similar to the calculation of active set PMF above, we calculate the mean power consumption of different power allocation schemes by using the probability distribution of joint pathloss difference. From (5.14), (5.15), (5.18), and (5.21), we find that the total power consumption of a mobile with different power allocation schemes ($\mathcal{P}_{LPPA}$, $\mathcal{P}_{SSDT}$, $\mathcal{P}_{EPA}$, and $\mathcal{P}_{QBPA}$) are functions of pathloss to base stations and thereby functions of L_k and $\boldsymbol{V}_k$. The mean power consumption of a mobile ($\overline{\mathcal{P}}$) with different power allocation schemes at a fixed point can be obtained by

$$\overline{\mathcal{P}} = \sum_{k=1}^{\Upsilon} \sum_{f=1}^{\Upsilon} \sum_{q=1}^{H_{k,f}} \overline{\mathcal{P}}_{k,f,q}, \tag{5.30}$$

where

$$\begin{aligned} & \overline{\mathcal{P}}_{k,f,q} \\ = & \int_{(0,\tau]^{f-1}} dv'_{k,f,q,1} \ldots dv'_{k,f,q,f-1} \int_{(\tau,\infty)^{\Upsilon-f}} dv'_{k,f,q,f} \ldots dv'_{k,f,q,\Upsilon-1} \\ & \frac{\exp\left\{-[\boldsymbol{V}'_{k,f,q} - \boldsymbol{P}_{k,f,q}\mathbf{U}_k]^T \boldsymbol{P}_{k,f,q}^{-T} \widehat{\mathbf{C}}_k^{-1} \boldsymbol{P}_{k,f,q}^{-1} [\boldsymbol{V}'_{k,f,q} - \boldsymbol{P}_{k,f,q}\mathbf{U}_k]/(2\sigma^2)\right\}}{\sqrt{(2\pi\sigma^2)^{\Upsilon-1} \det[\boldsymbol{P}_{k,f,q} \widehat{\mathbf{C}}_k \boldsymbol{P}_{k,f,q}^T]}} \mathcal{P}(L_k, \boldsymbol{V}'_{k,f,q}). \end{aligned} \tag{5.31}$$

The $\mathcal{P}(L_k, \boldsymbol{V}'_{k,f,q})$ in (5.31) can be substituted by $\mathcal{P}_{LPPA}$, $\mathcal{P}_{SSDT}$, $\mathcal{P}_{EPA}$, or $\mathcal{P}_{QBPA}$ to obtain the mean power consumption of a mobile at a fixes location with different power allocation mechanisms.

5.4 Outage probability

This section discusses the effects of fast fading on the different power allocation strategies in terms of outage probability performance. We analyze the outage probability due to Rician fast fading considering co-channel interference when applying different power allocation schemes, including EPA, QBPA, SSDT and LPPA.

5.4.1 Single Link Case (SSDT)

To begin with, we analyze the outage probability due to fast fading of single link case without maintaining the active set (not SSDT). We consider a system with Rician distributed received desired-signal power and Rayleigh distributed interfering-signal power. The outage probability for single link case without maintaining active set, is defined as

$$\begin{aligned} \mathrm{P}_{out}^{sl}(\eta) &= \mathrm{Prob}\left[(\frac{p_d}{p_I}) < \eta\right] \\ &= 1 - \int_0^{\infty} \left[\int_{-\infty}^{\frac{x}{\eta}} f_{p_I}(y)dy\right] d_{p_d}(x)dx \ , \end{aligned} \tag{5.32}$$

where p_d is the desired signal power with pdf f_{p_d}, p_I is the interfering signal power with pdf f_{p_I}, and η is the minimal required SIR. Denote Ω_d as the local mean power of the desired signal, $\underline{\Omega_I}$ as the local mean power of interfering signal where $\underline{\Omega_I} = \{\Omega_{I,i}\}_{i=1}^{\Upsilon}$ and $\Omega_{I,i}$ is the local mean interfering signal for base station i. Note that Ω_d and $\underline{\Omega_I}$ are log normally distributed because of the slow fading. The pdf of Ω_d is

$$f_{\Omega_d}(y) = \frac{1}{\sqrt{2\pi}\sigma_d y} \exp\left[\frac{-(\ln y - \ln \mu_d)^2}{2\sigma_d^2}\right] \ . \tag{5.33}$$

Assume the Ω_d and $\underline{\Omega_I}$ are given, and substitute (5.4) into (5.32). According to [38], we obtain

$$\mathrm{P}_{out}^{sl}(\eta|\Omega_d, \underline{\Omega_I}) = \sum_{i=1}^{\Upsilon} \frac{\Omega_{I,i}^{\Upsilon-1}}{\prod_{j=1,j\neq i}^{\Upsilon}(\Omega_{I,i} - \Omega_{I,j})} \frac{K_d + 1}{K_d + 1 + \frac{\Omega_d}{\eta\Omega_{I,i}}} \exp\left[\frac{-K_d\frac{\Omega_d}{\eta\Omega_{I,i}}}{K_d + 1 + \frac{\Omega_d}{\eta\Omega_{I,i}}}\right] \ , \tag{5.34}$$

where K_d is Rice factor of the desired signal. Assume $\{\Omega_{I,i}\}_{i=1}^{\Upsilon}$ are independent, the joint pdf of $\underline{\Omega_I}$ is

$$f_{\underline{\Omega_I}}(\underline{x}) = \prod_{i=1}^{\Upsilon} \frac{1}{\sqrt{2\pi}\sigma_{I,i}x_i} \exp\left[\frac{-(\ln x_i - \ln \mu_{I,i})^2}{2\sigma_{I,i}^2}\right] \ , \tag{5.35}$$

where $\underline{x} = (x_1, \cdots, x_\Upsilon)$. By combining (5.33), (5.34), and (5.35), we have

$$\begin{aligned} \mathrm{P}_{out}^{sl}(\eta) &= \int_0^\infty \cdots \int_0^\infty \mathrm{P}_{out}^{sl}(\eta|\Omega_d, \underline{\Omega}_I) f_{\Omega_d}(y) f_{\underline{\Omega}_I}(\underline{x}) dy d\underline{x} \\ &= \int_0^\infty \cdots \int_0^\infty \mathrm{P}_{out}^{sl}(\eta|\Omega_d, \underline{\Omega}_I) \cdot \frac{1}{\sqrt{2\pi}\sigma_d y} \exp\left[\frac{-(\ln y - \ln \mu_d)^2}{2\sigma_d^2}\right] \\ &\quad \cdot \prod_{i=1}^{\Upsilon} \frac{1}{\sqrt{2\pi}\sigma_{I,i} x_i} \exp\left[\frac{-(\ln x_i - \ln \mu_{I,i})^2}{2\sigma_{I,i}^2}\right] dy d\underline{x} \ , \end{aligned} \tag{5.36}$$

By using the substitution

$$\Theta = \ln(\Omega_d/\mu_d)/(\sqrt{2\pi}\sigma_d) \tag{5.37}$$

and

$$\Psi_i = \ln(\Omega_{I,i}/\mu_{I,i})/(\sqrt{2\pi}\sigma_{I,i}) \ , \tag{5.38}$$

where $i = 1, \cdots, \Upsilon$, we transform (5.36) into a Hermite integration form [39], which can be evaluated with numerical ease. In particular,

$$\begin{aligned} \mathrm{P}_{out}^{sl}(\eta)) &= \int_0^\infty \cdots \int_0^\infty \frac{\mathrm{G}(\Theta, \underline{\Psi})}{\sqrt{\pi}^{\Upsilon+1}} \exp\left[-\Theta^2 - \sum_{i=1}^{\Upsilon} \Psi_i^2\right] d\Theta d\underline{\Psi} \\ &\simeq \sum_{k_\Upsilon=1}^{h_\Upsilon} \cdots \sum_{k_0=1}^{h_0} \frac{\mathrm{G}(x_{k_0}, x_{k_1} \cdots, x_{k_\Upsilon})}{\sqrt{\pi}^{\Upsilon+1}} w_{k_0} \cdots w_{k_\Upsilon} \ , \end{aligned} \tag{5.39}$$

where $\underline{\Psi} = (\Psi_1, \cdots, \Psi_\Upsilon)$, x_{k_i} is the root of the h_ith order Hermite polynomial, and w_{k_i} is its corresponding weight factor. Here $\mathrm{G}(\Theta, \underline{\Psi})$ is obtained by substituting

$$\Omega_d = \mu_d \exp \sqrt{2}\Theta\sigma_d \tag{5.40}$$

and

$$\Omega_{I,i} = \mu_{I,i} \exp \sqrt{2}\Psi\sigma_{I,i} \ , \tag{5.41}$$

where $i = 1, \cdots, \Upsilon$, into $\mathrm{P}_{out}^{sl}(\eta|\Omega_d, \underline{\Omega}_I)$ in (5.34). That is

$$\mathrm{G}(\Theta, \underline{\Psi}) = \sum_{i=1}^{\Upsilon} \frac{1}{\prod_{j=1, j\neq i}^{\Upsilon} \{1 - \frac{\mu_{I,j}}{\mu_{I,i}} \exp[\sqrt{2}(\Psi_j \sigma_{I,j} - \Psi_i \sigma_{I,i})]\}} \frac{K_d + 1}{K_d + 1 + \epsilon_i} \exp\left[\frac{-K_d \epsilon_i}{K_d + 1 + \epsilon_i}\right] , \tag{5.42}$$

where

$$\epsilon_i = \frac{\mu_d}{\eta \mu_{I,i}} \exp[\sqrt{2}(\Theta \sigma_d - \Psi_i \sigma_{I,i})] . \tag{5.43}$$

The SSDT scheme also belongs to the single link case, but SSDT maintains active set. When applying the SSDT scheme, the mobile selects the best base station in the active set. Therefore, we have to slightly modify the outage probability of the SSDT as

$$\mathrm{P}_{out}^{sl}(\eta)_{SSDT} = \sum_{k=1}^{\Upsilon} \sum_{f=1}^{\Upsilon} \sum_{q=1}^{H_{k,f}} \mathrm{Prob}\left[(\frac{p_k}{p_I}) < \eta\right] Prob\{\boldsymbol{M}_{k,f,q}\} . \tag{5.44}$$

We obtain the outage probability by combining (5.39) and (5.44).

5.4.2 Multiple Links Case (LPPA, EPA, and QBPA)

In the previous subsection, we have derive a close-form expression for outage probability due to Rician fading in the single link case, i.e. there is only one base station in the active set. Here, we would like to extend the single link case to the multiple links case. First, we define the outage probability of multiple links case as

$$\begin{aligned} \mathrm{P}_{out}^{ml}(\eta) &= \mathrm{Prob}\left[\sum_{i \in M} (\frac{p_d}{p_I})_i < \eta\right] \\ &= \sum_{k=1}^{\Upsilon} \sum_{f=1}^{\Upsilon} \sum_{q=1}^{H_{k,f}} \mathrm{Prob}\left\{\sum_{i \in \boldsymbol{M}_{k,f,q}} (\frac{p_d}{p_I})_i < \eta\right\} \cdot Prob\{\boldsymbol{M}_{k,f,q}\} , \end{aligned} \tag{5.45}$$

where $(p_d/p_I)_i$ is the SIR of link to base station i and the probability of $\boldsymbol{M}_{k,f,q}$ is derived in (5.28). Assume $\{(p_d/p_I)_i\}_{i=1}^{f}$ are independent, we rewrite the first term of

right hand side of (5.45) as

$$
\begin{aligned}
& \text{Prob}\left[(\frac{p_d}{p_I})_1 + \ldots + (\frac{p_d}{p_I})_f < \eta\right] \\
= & \int_0^{\eta} d\eta_{f-1} \int_0^{\eta-\eta_{f-1}} d\eta_{f-2} \cdots \int_0^{\eta-\eta_{f-1}\cdots\eta_2} d\eta_1 \\
& \cdot\text{Prob}\left\{(\frac{p_d}{p_I})_1 < \eta_1 \mid \left[(\frac{p_d}{p_I})_2 + \ldots + (\frac{p_d}{p_I})_f < \eta - \eta_1\right]\right\} \\
& \cdot\text{Prob}\left\{(\frac{p_d}{p_I})_2 < \eta_2 \mid \left[(\frac{p_d}{p_I})_3 + \ldots + (\frac{p_d}{p_I})_f < \eta - \eta_1 - \eta_2\right]\right\} \cdots \\
& \cdot\text{Prob}\left\{(\frac{p_d}{p_I})_{f-1} < \eta_{f-1} \mid \left[(\frac{p_d}{p_I})_f < \eta - \eta_1 - \cdots \eta_{f-1}\right]\right\} \\
& \cdot\text{Prob}\left\{(\frac{p_d}{p_I})_f < \eta - \eta_1 - \cdots \eta_{f-1}\right\} \\
= & \int_0^{\eta} d\eta_{f-1} \int_0^{\eta-\eta_{f-1}} d\eta_{f-2} \cdots \int_0^{\eta-\eta_{f-1}\cdots\eta_2} d\eta_1 \text{Prob}\left[(\frac{p_d}{p_I})_1 < \eta_1\right] \text{Prob}\left[(\frac{p_d}{p_I})_2 < \eta_2\right] \\
& \cdots\text{Prob}\left[(\frac{p_d}{p_I})_{f-1} < \eta_{f-1}\right] \text{Prob}\left[(\frac{p_d}{p_I})_f < \eta - \eta_1 - \cdots \eta_{f-1}\right] \quad , \qquad (5.46)
\end{aligned}
$$

where $\eta_1, \cdots, \eta_{f-1}$ are dummy variables. By substituting outage probability expression for single link of (5.39) into (5.45) and (5.46), we obtain the outage probability for multiple links case.

Power allocation mechanism calculate the transmission power of each base station in the active set based on the path loss and log normal shadowing. Different power allocation scheme leads to different $p_{d,i}$ of (5.45) thereby change the sensitivity to fast fading. Take LPPA as an example, the received signal power from base station i (denoted as $p_{d,i}$) can be obtained from (5.13). Specifically,

$$
p_{d,i} = \frac{\widehat{p}_{i,LPPA}}{L_i} = \frac{SIR_{req}}{L_i \sum_{j=1}^{f} \frac{1/L_j}{AL_j - B}} \frac{1}{L_i} \quad , \qquad (5.47)
$$

where $\widehat{p}_{i,LPPA}$ is the power transmitted from base station i based on LPPA. Assume all the base stations transmit their maximum amount of power, i.e. $P_i = P_{max}$, $i = 1 \cdots \Upsilon$, in (5.9). Then, the only random variable in (5.47) is L, which is log normally distributed. By using the Fenton-Wilkinson's approximation [36], we approximate the sum of log-normal random variables as another log-normal random variable. That is

$$e^{\psi} = \sum_{i=1}^{M} e^{\zeta_i}, \tag{5.48}$$

where both ψ and ζ are normal distributed, and the mean of ψ is

$$\mu_{\psi} = 2\ln(u_1) - \frac{1}{2}\ln(u_2), \tag{5.49}$$

and its variance is

$$\sigma_{\psi}^2 = 2\ln(u_2) - 2\ln(u_1). \tag{5.50}$$

Note that in (5.49) and (5.50),

$$u_1 = \sum_{i=1}^{M} e^{\mu_{\zeta_i} + \sigma_{\zeta_i}^2/2} \tag{5.51}$$

and

$$\begin{aligned} u_2 &= \sum_{i=1}^{M} e^{2\mu_{\zeta_i} + 2\sigma_{\zeta_i}^2} \\ &\quad + 2\sum_{i=1}^{M-1}\sum_{j=i+1}^{M} \{e^{\mu_{\zeta_i} + \mu_{\zeta_j}} \cdot e^{\frac{1}{2}(\sigma_{\zeta_i}^2 + \sigma_{\zeta_j}^2 + 2r_{ij}\sigma_{\zeta_i}\sigma_{\zeta_j})}\}. \end{aligned} \tag{5.52}$$

The $p_{d,i}$ of (5.47) can be approximated as a new log normal variable with mean $\mu_{d,i,LPPA}$ and standard deviation $\sigma_{d,i,LPPA}$. Similarly, the received power from base station i by using other multiple link power allocation schemes, such as EPA and QBPA, can also be approximated as log normal variables with mean and standard

deviation $\mu_{d,i,EPA}$, $\sigma_{d,i,EPA}$, $\mu_{d,i,QBPA}$, and $\sigma_{d,i,QBPA}$, respectively. By substituting $\mu_{d,i,LPPA}$, $\sigma_{d,i,LPPA}$, $\mu_{d,i,EPA}$, $\sigma_{d,i,EPA}$, $\mu_{d,i,QBPA}$, and $\sigma_{d,i,QBPA}$ into μ_d and σ_d of (5.40), we introduce the effects of different power allocation schemes into our analysis of multi-link outage due to fast fading.

5.5 Numerical Results

In this section, we give some numerical results of power efficiency and outage probability due to Rician fast fading for different power allocation schemes, including LPPA, SSDT, EPA and QBPA. Through analysis provided in Section 5.3, we can evaluate the impacts of key system parameters on system performance, including orthogonality factor α and soft handoff threshold τ.

5.5.1 Power Efficiency Comparison

We provide the numerical results of the power efficiency for different power allocation schemes according (5.30) (5.31) in Section 5.3. Figure 1 shows a two-cell layout with a mobile moving from cell A to cell B. Let the standard deviation of log normal shadowing to 8 dB, the orthogonality factor α be 0.4, the soft handoff threshold τ be 9 dB, SIR requirement to be -10 dB, and the base station radius to be 1000 meeters. Figure 2 shows the total power consumption for a mobile with different power allocation schemes at different locations. As we can see in Figure 2, the average consumed power at the cell boundary for SSDT, LPPA, EPA, and QBPA are 1333, 1510, 1767, and 2480 milliwatts, respectively. SSDT is the most power efficient power allocation schemes, while QBPA performs worst. We also provide the pure simulation results of SSDT and LPPA cases to verify our analytical values. Figure 3 shows the power consumption of different power allocation schemes if we change

the orthogonality factor α to be 0.2, and the soft handoff threshold τ to be 3 dB. In this case, the power consumed by the mobile at the cell boundary with SSDT, LPPA, EPA, and QBPA are 933, 1001, 1026, and 1057 milliwatts, respectively. Notice that the power consumed by a mobile with different power allocation schemes differs most at the cell boundary. Because the consumed power difference among different power allocation schemes occurs only when the mobile is in the handoff process and the handoff probability is highest at cell boundary.

5.5.2 Impacts of Handoff Threshold and Orthogonality Factor

Figures 4 and 5 illustrate the impact of orthogonality factor α at the middle point of two base stations (distance to base station 1 is 1000 meters) with soft handoff threshold τ equal to 6 dB and 3 dB, respectively. A orthogonality factor consumes more power in all power allocation schemes. Comparing Fig. 4 and Fig. 5, it is shown that the larger handoff threshold enlarges the difference of power consumption of four power allocations.

In Figure 6, we fix the orthogonality to be 0.2 and illustrate the impact of soft handoff threshold with different power allocation schemes. Different power allocation schemes has different sensitivity to the change of soft handoff threshold. The power consumption of SSDT almost remains constant in all all values of soft handoff threshold, while the power consumed of the other three power allocation schemes increases in different degrees as soft handoff threshold increases. The QBPA is most sensitive to the change of soft handoff threshold, and the SSDT is the least sensitive one.

5.5.3 Effects of Fast Fading

Figures 7 and 8 compare the outage probability due to Rician fading when applying different power allocation schemes. These numerical results are obtained when the handoff threshold τ is set to be 3 dB, η is set to be -14 dB, and the Rice factors are set to be 3 dB and 10 dB, respectively. As shown in the figures, SSDT suffers the highest outage probability due to Rician fading, while QBPA is least sensitive to the Rician fading effects. The outage probability decreases when the mobile moves to the cell boundary when applying multi-link power allocation schemes (EPA, QBPA, and LPPA), because the soft handoff probability increases near cell boundary and the soft handoff mechanism ease the instantaneous SIR shortage due to Rician fading. The outage probability of the single-link power allocation scheme (SSDT) and the multi-link power allocation schemes (EPA, QBPA, and LPPS) differ most at cell boundary. The outage probability difference is equal to 4.5% at cell boundary.

5.6 Conclusions

In this chapter, we have derived the closed-form expressions for the consumed power and outage probability due to fast fading effects. Both co-channel interference and different power allocation schemes are taken into consideration. We consider four power allocation schemes, including equal power allocation (EPA), quality balancing power allocation (QBPA), site selection diversity transmission (SSDT), and link proportional power allocation (LPPA) mechanisms. According to our numerical result, SSDT is most power efficient, but it suffers highest sensitivity to Rician fading effects. As compared to the SSDT method, the LPPA mechanism achieves better outage in presence of fast fading at the cost of slightly sacrificing power efficiency.

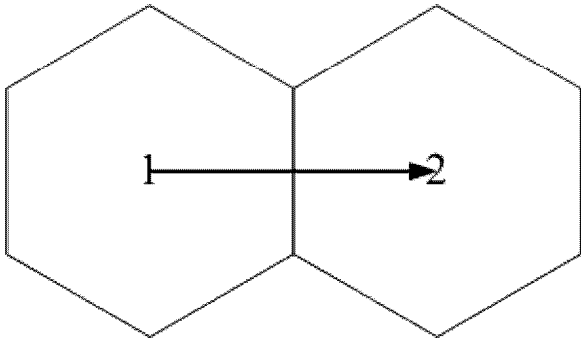

Figure 5.1: A two-cell base station layout.

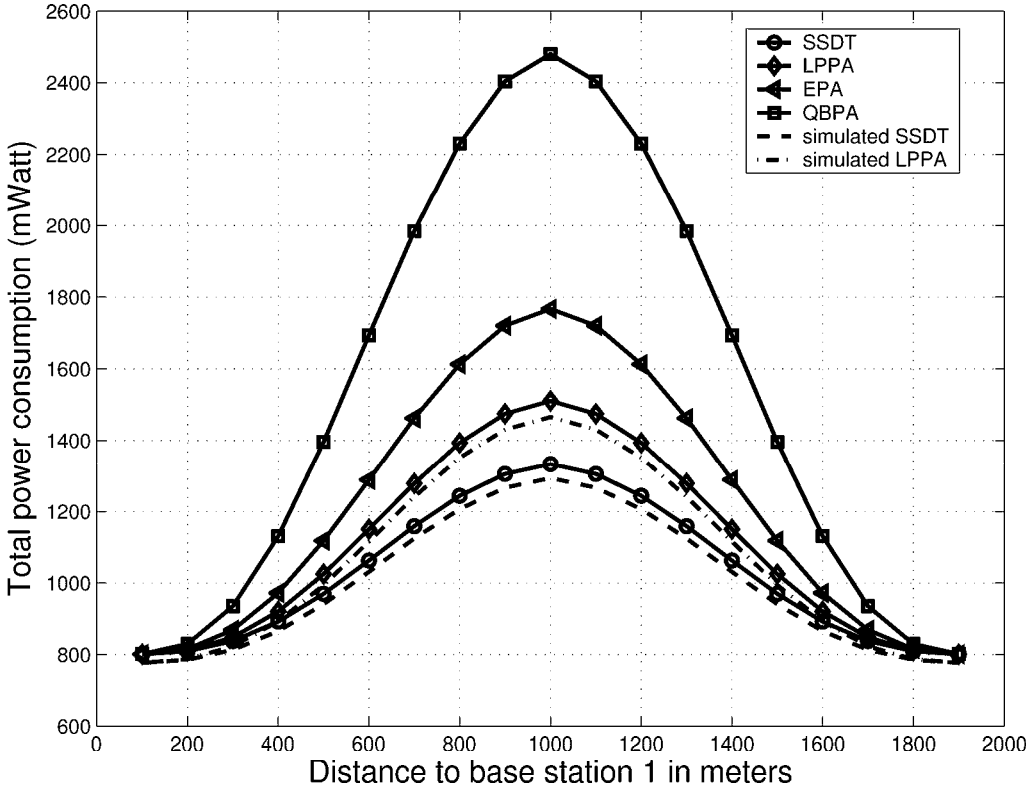

Figure 5.2: Comparison of the required transmission power for different power allocation schemes at different locations, where $SIR_{req} = -10$ dB, $\alpha = 0.4$, and $\tau = 9$ dB.

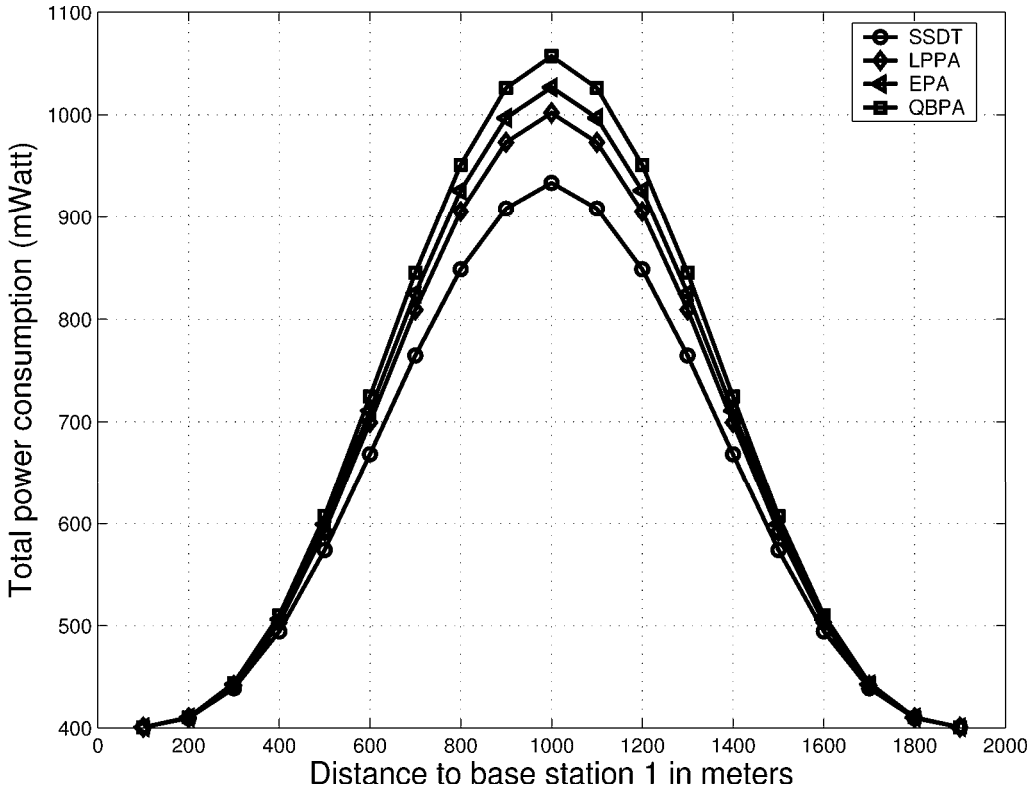

Figure 5.3: Comparison of the required transmission power for different power allocation schemes at different locations, where $\alpha = 0.2$, and $\tau = 3$ dB.

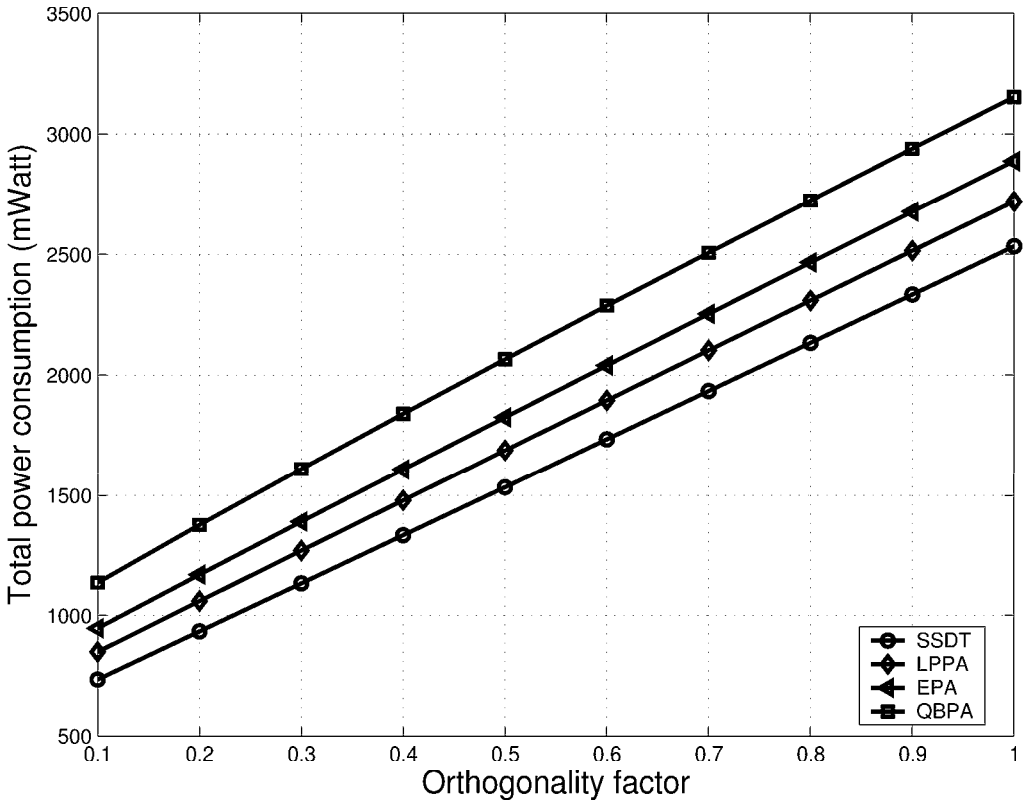

Figure 5.4: Effect of orthogonality factor on the required transmission power for different power allocation stategies during soft handoff, where $\tau = 6$ dB.

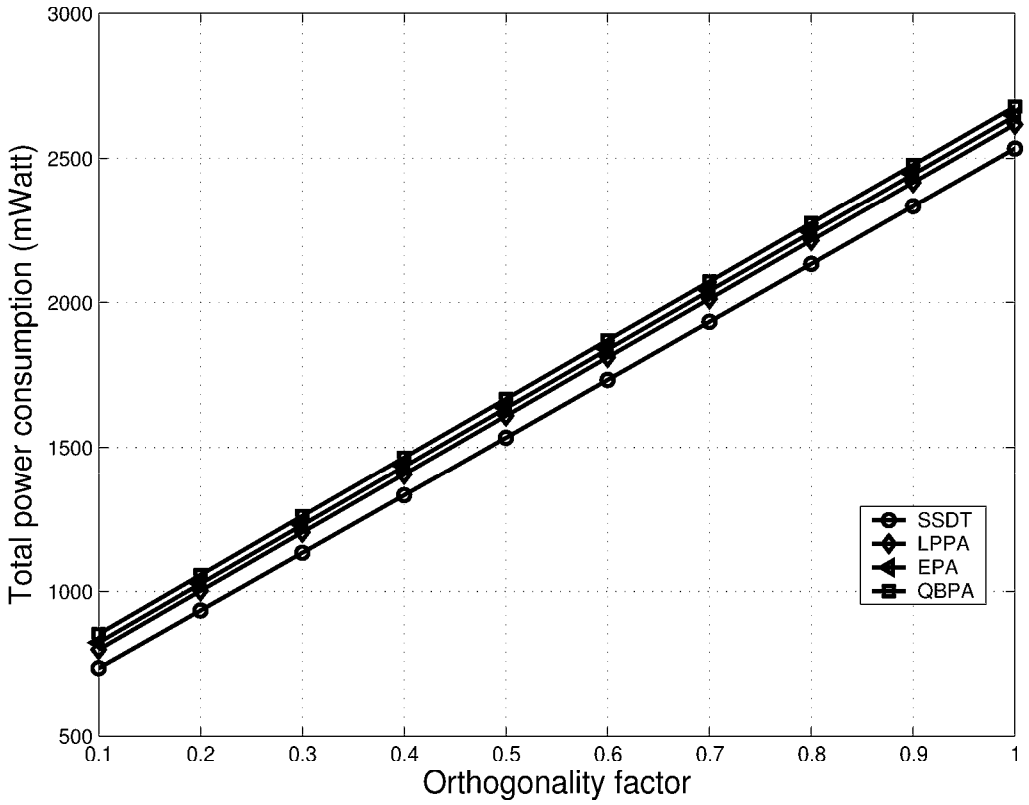

Figure 5.5: Effect of orthogonality factor on the required transmission power for different power allocation stategies during soft handoff, where $\tau = 3$ dB.

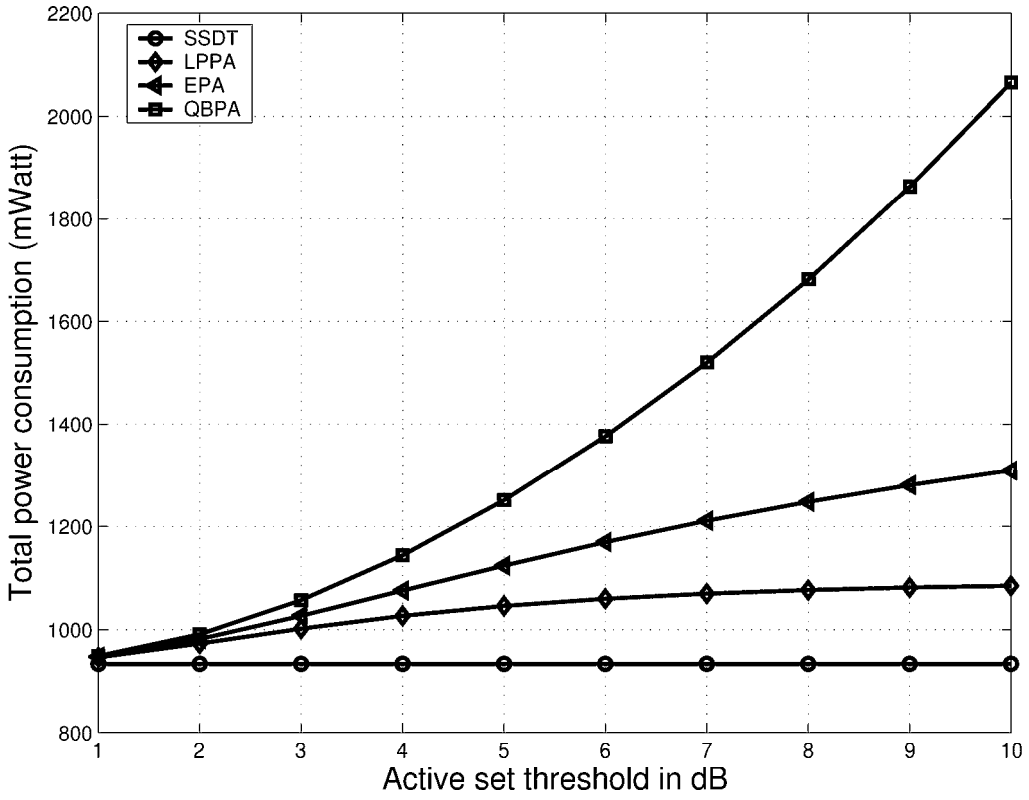

Figure 5.6: Effect of handoff threshold on the required transmission power for different power allocation stategies during soft handoff, where $\alpha = 0.2$ dB.

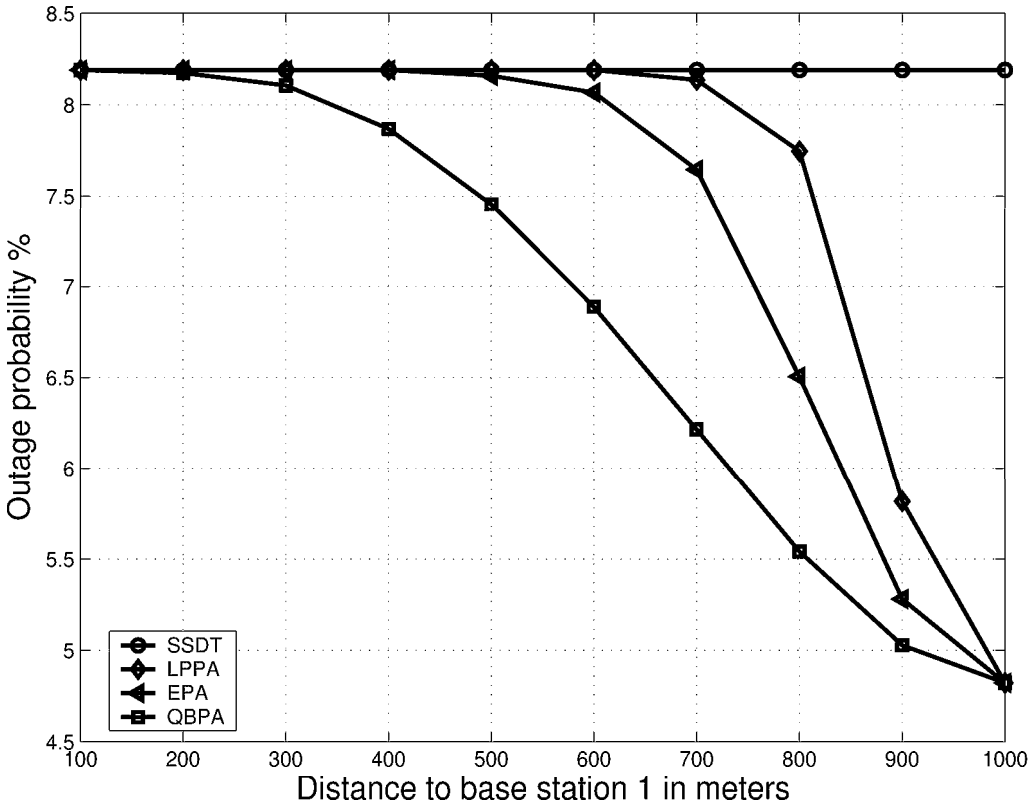

Figure 5.7: Comparison of outage probability due to Rician fast fading with Rice factor $K_d = 3$ dB.

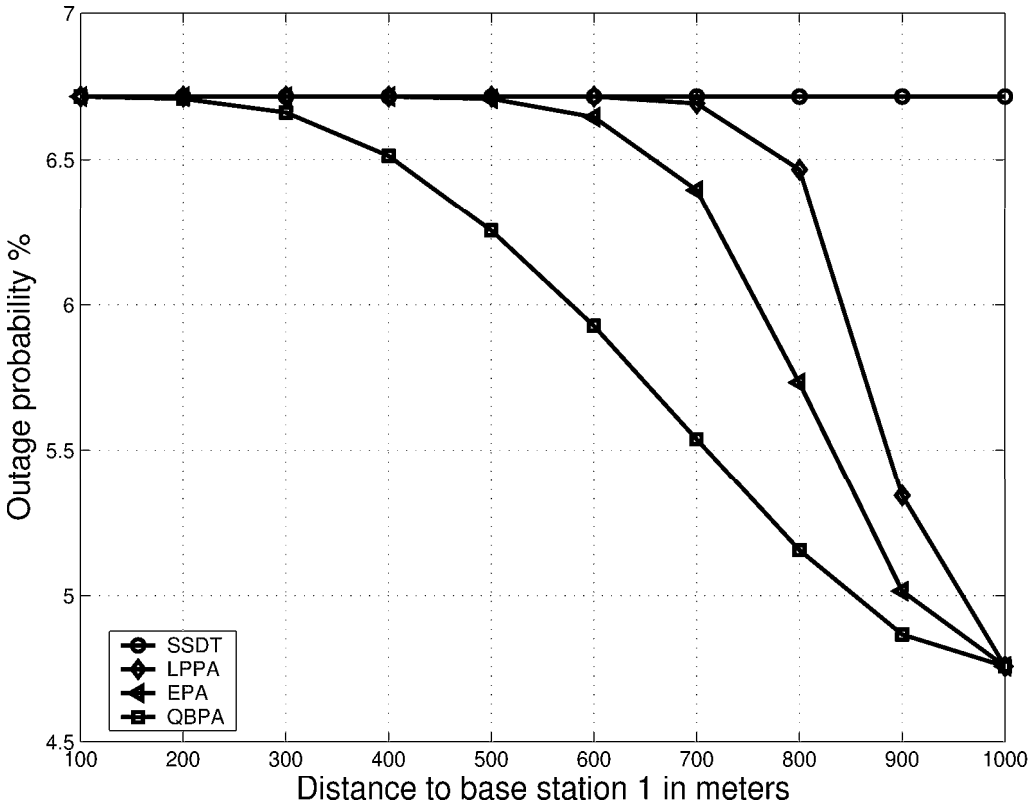

Figure 5.8: Comparison of outage probability due to Rician fast fading with Rice factor $K_d = 10$ dB.

CHAPTER 6

Concluding Remarks

The objective of this thesis is to evaluate the performance of downlink power allocation mechanisms and soft handoff for supporting high bit rate multimedia services in WCDMA systems. This thesis includes the following topics:

1. A Contour Overlapping Technique for Soft Handover Parameters Design in the WCDMA System;

2. Performance Evaluation of Downlink Power Allocation Mechanisms for Soft Handoff in the WCDMA System with Power Control Errors;

3. Performance Analysis of Downlink Power Allocation Mechanisms for Soft Handoff in the WCDMA System with Co-channel Interference.

Contributions from this research are listed as follows.

1. Present a contour overlapping technique to design downlink soft handoff parameters setting for the WCDMA system. The proposed methodology focuses on two parameters (AS_TH and AS_TH_Hyst), which influence the system performance more significant than the other parameters. The optimal parameters achieving multiple system requirements can be designed systematically by the proposed methodology.

2. Evaluate the outage probabilities of different power allocation mechanisms subject to transmission power control errors and base station power shortage by a

semi-analytical approach. The proposed LPPA has better outage performance compared to SSDT with moderate load considering the joint effect of power control errors and base station power shortage.

3. Present an analytical approach to evaluate the outage probability of a handoff user in the WCDMA system when applying different downlink power allocation mechanisms in the log-normally shadowed and Rician fading channel subject to co-channel interference. An analytical formula for calculating the power efficiency of different power allocation schemes is also derived in this chapter.

The following summarizes the results from the above contributions.

6.1 A Contour Overlapping Technique for Soft Handover Parameters Design in the WCDMA System

In Chapter 3 and [24], we have discussed the impact of the soft handoff parameters with respect to the WCDMA system. We find that only two parameters, i.e. AS_TH and AS_TH_HYST, affect the system performance significantly. Based on this observation, we propose a contour overlapping technique to simplify soft handoff parameters design with emphasis on the setting of AS_TH and AS_TH_HYST. By using the proposed methodology, we can easily find the optimal handoff parameters subject to different performance requirements. Thus the proposed handoff parameter design approach can be used to optimize the performance for the WCDMA system.

6.2 Performance Evaluation of Downlink Power Allocation Mechanisms for Soft Handoff in the WCDMA System with Power Control Errors

In Chapter 4 and [35], we have investigated the performance of different downlink power allocation schemes for soft handoff in CDMA systems subject to power control errors. With consideration of both base station power shortage and power control errors, we analyze the outage and capacity performances of equal power allocation (EPA), quality balancing power allocation (QBPA), site selection diversity transmission (SSDT), and link proportional power allocation (LPPA) mechanisms.

The contribution of this work are three folds. First, we apply a harmonic-arithmetic mean inequality and Chebyshev inequality to prove that SSDT is the most efficient power allocation mechanism as compared to other schemes, such as EPA, QBPA, and LPPA schemes. Secondly, we further derive the closed-form expressions for the outage probabilities of different power allocation mechanisms subject to transmission power control errors. Third, from both the perspectives of base station power shortage and power control errors, we develop a semi-analytical approach to evaluate the outage performance of different power allocation schemes. Our numerical results demonstrate that due to power control errors the SSDT system suffers from a higher outage probability in the moderate traffic load condition although it can achieve the best outage probability performance in the heavy traffic condition. Furthermore, we show that the LPPA system can almost approach the capacity of the SSDT system, while maintaining lower outage probability than SSDT in the moderate traffic.

6.3 Performance Analysis of Downlink Power Allocation Mechanisms for Soft Handoff in the WCDMA System with Co-channel Interference

In Chapter 5 and [40], we have derived the closed-form expressions for the consumed power and outage probability due to fast fading effects. Both co-channel interference and different power allocation schemes are taken into consideration. We consider four power allocation schemes, including EPA, QBPA, SSDT, and LPPA mechanisms. According to our numerical result, SSDT is most power efficient, but it suffers highest sensitivity to Rician fading effects. As compared to the SSDT method, the LPPA mechanism achieves better outage in presence of fast fading at the cost of slightly sacrificing power efficiency.

6.4 Suggestions for Future Research

6.4.1 A Contour Overlapping Technique for Soft Handover Parameters Design in the WCDMA System

In this work, we have developed a wireless network dynamic simulation platform (WINDSP) to evaluate the performance of soft handoff algorithm. To enhance the quality of WINDSP is an interesting extension work for future. More functions can be included into the WINDSP, such as the the impacts of multi-rate demanding users, realistic data traffic model, and different power allocation schemes.

6.4.2 Performance Evaluation of Downlink Power Allocation Mechanisms for Soft Handoff in the WCDMA System with Power Control Errors

We have evaluated the four power allocation schemes from the standpoint of power efficiency and sensitivity to power control errors with predefined soft handoff parameters. How to determine the optimal soft handoff parameter when applying different power allocation schemes is an interesting topic for future research.

6.4.3 Performance Analysis of Downlink Power Allocation Mechanisms for Soft Handoff in the WCDMA System with Co-channel Interference

We have analyzed three outage-resulting factors in Chapters 4 and 5, including base station power shortage, power control errors, and fast fading effects. The joint effects of the three factors when applying different power allocation schemes may be an interesting topic for the future research.

Bibliography

[1] T. S. Rappaport, *Wireless Communications- Principles and practice.* Prentice Hall PTR Co., 2002.

[2] E. Dahlman, P. Beming, J. Knutsson, F. Ovesjo, M. Persson, and C. Roobol, "WCDMA-the radio interface for future mobile multimedia communications," *IEEE Transactions on Vehicular Technology*, vol. 47, pp. 1105–1118, Nov. 1998.

[3] T. Ojanpera and R. Prasad, "An overview of third-generation wireless personal communications: a european perspective," *IEEE Personal Communications*, pp. 59–65, Dec. 1998.

[4] N. D. Tripathi, J. H. Reed, and H. F. VanLandinoham, "Handoff in cellular systems," *IEEE Personal Communications*, pp. 26–37, Dec. 1998.

[5] A. F. Molisch, *Wideband wireless digital communications.* Prentice Hall PTR Co., 2001.

[6] J. Zander and S. L. Kim, *Radio resourece management for wireless networks.* Artech House Co., 2001.

[7] K. Pahlavan and P. Krishnamurthy, *Priciples of wireless networks.* Prentice Hall PTR Co., 2002.

[8] K. S. Gilhousen, "On the capacity of a cellular CDMA system," *IEEE Transactions on Vehicular Technology*, vol. 40, pp. 303–312, May 1991.

[9] A. J. Viterbi and A. M. Viterbi, "Erlang capacity of a power controlled CDMA system," *IEEE Journal on Selected Areas in Communications*, pp. 892–900, Aug. 1993.

[10] Y. P. E. Wang and G. E. Bottomley, "CDMA downlink system capacity enhancement through generalized RAKE reception," in *Proceedings of IEEE Vehicular Technology Conference*, Oct. 2001, pp. 1177–1181.

[11] K. Kettunen, "Enhanced maximal ratio combining scheme for rake receivers in wcdma mobile terminals," *IEEE Electronics Letters*, pp. 522–524, Apr. 2001.

[12] K. Heck, D. Staehle, and K. Leibnitz, "Diversity effects on the soft handover gain in UMTS networks," in *Proceedings of IEEE Vehicular Technology Conference*, Sep. 2002, pp. 1269–1273.

[13] N. Binucci, K. Hiltunen, and M. Caselli, "Soft handover gain in WCDMA," in *Proceedings of IEEE Vehicular Technology Conference*, Sep. 2000, pp. 1467–1472.

[14] H. Furukawa, K. Harnage, and A. Ushirokawa, "SSDT-site selection diversity transmission power control for CDMA forward link," *IEEE Journal on Selected Areas in Communications*, pp. 1546–1554, Aug. 2000.

[15] P. Coulon and S. Vadgama, "Performance of site selection diversity transmission in WCDMA," in *Proceedings of International Symposium on Wireless Personal Multimedia Communications Conference*, Oct. 2002, pp. 72–76.

[16] J. Hamalainen and R. Wichman, "On the site selection diversity transmission," in *Proceedings of Personal, Indoor and Mobile Radio Communications*, Sep. 2003, pp. 1031–1035.

[17] D. Staehle, K. Leibnitz, and K. Heck, "Effects of soft handover on the UMTS downlink performance," in *Proceedings of IEEE Vehicular Technology Conference*, Sep. 2002, pp. 960–964.

[18] L. C. Wang, C. Y. Liao, and C. J. Chang, "Downlink soft handoover and power allocation for CDMA heterogeneous cellular network," in *Proceedings of IEEE Global Telecommunications Conference*, Nov. 2002, pp. 1830–1836.

[19] L. C. Wang, M. C. Chiang, L. Chen, C. J. Chang, and C. Y. Liao, "Performance comparisons of power allocation mechanisms for downlink handoff in the WCDMA system with microcellular environments," in *Proceedings of ACM International Workshop on Modeling, Analysis, and Simulation of Wireless and Mobile Systems*, Sep. 2003.

[20] A. J. Viterbi, CDMA*: Priciples of Spread Spectrum communication.* Addison-Wesley Publishing Co., 1995.

[21] D. Avitor, N. Hegde, and S. Mukherjee, "Impact of soft handoff threshold and maximum active group size on base station downlink transmission power in UMTS system," in *Proceedings of IEEE Vehicular Technology Conference*, Apr. 2003, pp. 1974–1978.

[22] 3GPP *Technical Specification Group, Radio Access Networks: Physical layer procedures (*FDD*).* 3G TS 25.214, Version 3.1.0, Dec. 1999.

[23] D. Kim, "A simple algorithm for adjusting cell-site transmitter power in CDMA cellular systems," in *Proceedings of IEEE Vehicular Technology Conference*, July 1999, pp. 1092–1098.

[24] L. C. Wang and L. Chen, "Contour overlapping technique for soft handover parameters optimization in the WCDMA system," in *Proceedings of International Symposium on Wireless Personal Multimedia Communications Conference*, Oct. 2003, pp. 549–553.

[25] 3GPP *Technical Specification Group, Radio Access Networks: Radio resource management strategies.* 3G TR 25.922, Version 3.1.0, Mar. 2000.

[26] S. J. Hong and I.-T. Lu, "Soft handoff algorithm parameter optimization in various propagation environments," in *Proceedings of IEEE Vehicular Technology Conference*, May 2001, pp. 2549–2553.

[27] Yang, Ghaheri-Niri, and Tafazolli, "UTRA soft handoff optimisation," in *Proceedings of 3G Mobile Communication Technologies International Conference*, May 2002, pp. 37–41.

[28] L.-C. Wang, "A new cellular architecture based on an interleaved cluster concept," *IEEE Transactions on Vehicular Technology*, pp. 1809–1818, Nov. 1999.

[29] 3GPP *Technical Specification Group, Radio Access Networks: Selection procedure for the choice of radio transmission technology.* 3G TR 101.112, Version 3.2.0, Apr. 1998.

[30] J. Laiho and A. Wacker, *Radio network planning and optimization for* UMTS. AJohn Wiley & Sons Co., 2002.

[31] 3GPP *Technical Specification Group, Radio Access Networks:* RRC *Protocol Specification.* 3G TS 25.331, Version 3.1.0, Jan. 2000.

[32] 3GPP *Technical Specification Group, Radio Access Networks: RF System Scenarios.* 3G TR 25.942, Version 2.3.0, Sep. 2000.

[33] A. J. Viterbi, A. M. Viterbi, K. S. Gilhousen, and E. Zehavi, "Soft handoff extends CDMA cell coverage and increases reverse link capacity," *IEEE Journal on Selected Areas in Communications*, pp. 1281–1288, Oct. 1994.

[34] D. Staehle, K. Leibnitz, K. Heck, B. Schroder, A. Weller, and P. Tran-Gia, "Analytical characterization of the soft handover gain in UMTS," in *Proceedings of IEEE Vehicular Technology Conference*, Oct. 2001, pp. 291–295.

[35] L. C. Wang and L. Chen, "Performance analysis of link proportional power allocation for downlink soft handoff in CDMA systems," in *Proceedings of IEEE Vehicular Technology Conference*, May. 2004.

[36] A. A. Abu-Dayya and N. C. Beaulieu, "Outage probabilities in the presence of correlated lognormal interferers," in *Proceedings of IEEE Vehicular Technology Conference*, Feb. 1994, pp. 164–173.

[37] D. Avidor, N. Hegde, and S. Mukherjee, "On the impact of the soft handoff threshold and the maximum size of the active group on resource allocation and outage probability in the UMTS system," *IEEE Wireless Communications*, pp. 565–577, Mar. 2004.

[38] L. C. Wang, G. L. Stuber, and C. T. Lea, "Effects of rician fading and branch correlation on a local-mean-based macrodiversity cellular system," *IEEE Transactions on Vehicular Technology*, vol. 31, pp. 429–436, Mar. 1999.

[39] J. P. Linnartz, *Narrowband Land-Mobile Radio Networks.* Artech House Co., 1993.

[40] L. C. Wang and L. Chen, "Performance analysis of downlink power allocation mechanisms for soft handoff in the wcdma system with co-channel interference," in *XXX (will be submitted soon).*

Vita

Lei Chen was born in Taiwan in 1980. He received a B.S. in the Department of Communication Engineering of National Chiao Tung University in 2002. From July 2002 to June 2004, he obtained his Master degree at the Wirelsss Network Lab in the Department of Communication Engineering of National Chiao Tung University. His research interests are in the field of wireless communications.